Bifurcation Analysis of a Predator-prey System with Generalised Holling Type III Functional Response*

Yann Lamontagne† Caroline Coutu‡ Christiane Rousseau§

December 19, 2007

Abstract

We consider a generalised Gause predator-prey system with a generalised Holling response function of type III: $p(x) = \frac{mx^2}{ax^2+bx+1}$. We study the cases where b is positive or negative. We make a complete study of the bifurcation of the singular points including: the Hopf bifurcation of codimension 1 and 2, the Bogdanov-Takens bifurcation of codimension 2 and 3. Numerical simulations are given to calculate the homoclinic orbit of the system. Based on the results obtained, a bifurcation diagram is conjectured and a biological interpretation is given.

1 Introduction

We consider a generalised Gause predator-prey system [15, 13] of the following form

$$\begin{cases} \dot{x} = rx\left(1 - \frac{x}{k}\right) - yp(x) \\ \dot{y} = y(-d + cp(x)) \\ x(0) > 0, y(0) > 0 \end{cases} \tag{1.1}$$

with a generalised Holling response function of type III

$$p(x) = \frac{mx^2}{ax^2 + bx + 1}. \tag{1.2}$$

The system has seven parameters, the parameters a, c, d, k, m and r are positive. We study the cases where b is positive or negative. The parameters a, b, m are fitting parameters of the response function. The parameter d is the death rate of the predator while c is the efficiency of the predator to convert prey into predators.

*This work was supported by NSERC in Canada.

†E-mail yann@daume.org.

‡Collège Édouard-Montpetit, e-mail caroline.coutu@college-em.qc.ca.

§Département de Mathématiques, Université de Montréal, C.P. 6128, Succursale Centre-ville, Montréal, Québec, H3C 3J7, CANADA, e-mail rousseac@dms.umontreal.ca.

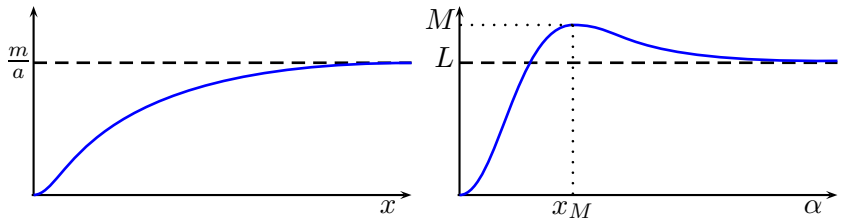

(a) $b \geq 0$ (b) $b < 0$

Figure 1.1: Generalised Holling type III functional response.

The prey follows a logistic growth with a rate r in the absence of predator. The environment has a prey capacity determined by k.

The case $b \geq 0$ has been studied biologically by Jost and al. in 1973 [19, 20]. The generalised Holling functional response of type III was used to model the predation of *Tetrahymena pyriformis* on *Escherichia coli* or *Azotobacter vinelandii* in a chemostat. The chemostat system with the generalised Holling response function of type III was used instead of the Holling response function of type II ($p(x) = \frac{bx}{1+ax}$) since the former response function gave better results. This is partly due to the rate of predation which does not diminish sufficiently fast in type II when the prey population tends to zero. Indeed, for type II (resp. III) the response function has a nonzero (resp. zero) slope at $x = 0$ (see Fig. 1(a)). We show that the case $b > 0$ is qualitatively equivalent to the case $b = 0$ (i.e. $p(x) = \frac{mx^2}{ax^2+1}$ also known as Holling response function of type III [18, 12]). A study of a predator-prey with a Holling response function of type IV, in a very similar spirit, was recently done by Broer-Naudot-Roussarie-Saleh (see [4, 5]).

The case $b < 0$ provides a model for a functional response with limited group defence. In opposition to the generalised Holling function of type IV ($p(x) = \frac{mx}{ax^2+bx+1}$) studied in [1, 4, 5, 14, 23, 22, 24] where the response function tends to zero as the prey population tends to infinity, the generalised function of type III tends to a nonzero value L as the prey population tends to infinity (see Fig. 1(b)). The functional response of type III with $b < 0$ has a maximum M at x_M. It is possible to obtain a, b, and m as functions of L, M and x_M. When studying the case $b < 0$ we will find a Bogdanov-Takens bifurcation of codimension 3 which is an organizing center for the bifurcation diagram.

The system (1.1) has 7 parameters but, with the following scaling $(X, Y, T) = (\frac{1}{k}x, \frac{1}{ck}y, cmk^2t)$ of the variables, we are able to reduce the number of parameters to 4. The system which we consider is

$$\begin{cases} \dot{x} = \rho x(1-x) - yp(x) \\ \dot{y} = y(-\delta + p(x)) \\ x(0) > 0, y(0) > 0 \end{cases} \tag{1.3}$$

where

$$p(x) = \frac{x^2}{\alpha x^2 + \beta x + 1} \tag{1.4}$$

and the parameters are $(\alpha, \beta, \delta, \rho) = (ak^2, bk, \frac{d}{cmk^2}, \frac{r}{cmk^2})$. The parameter space is of dimension 4 but we noticed that all but the homoclinic orbit bifurcation and the bifurcation of the double limit cycle do not depend on the ρ parameter. Therefore the bifurcation diagrams are given in the (α, δ) plane for values of β. The values of β are either generic or bifurcation values.

The article is organized as follows: in section 2 we show that all trajectories are attracted to a finite region of the plane. In section 3 we study the number of singular points. In section 4 we study the saddle/anti-saddle character of the singular points. In section 5 we discuss the Bogdanov-Takens bifurcation of codimension 2 and 3. In section 6 we study the Hopf bifurcation of codimension 1 and 2. In section 7 a bifurcation diagram is conjectured. The proposed bifurcation diagram is the simplest which extends the local bifurcations surfaces and curves in the neighborhood of the Bogdanov-Takens bifurcations and takes into account the saddle-node bifurcation where the saddle point exits the first quadrant: hence the Bogdanov-Takens bifurcation of codimension 3 is really an organizing center for the bifurcation diagram. Finally in section 8 we study the homoclinic bifurcation by numerical simulation and find necessary conditions for the existence of a homoclinic orbit. We discuss in section 9 a biological interpretation.

2 Behaviour of trajectories at infinity

In this section we show that all trajectories are attracted to a finite region of the plane.

Theorem 2.1 *For any parameter values $(\alpha, \beta, \delta, \rho)$ there exists a box $B = [0, 1] \times [0, R]$, where $R = R(\alpha, \beta, \delta, \rho)$ such that all trajectories in the first quadrant have their ω-limit set inside B.*

Proof. Since $\dot{x} < 0$ for $x > 1$ all trajectories enter inside the region $x \leq 1$. This occurs in a finite time as soon as $y(t)$ remains bounded away from 0. Moreover $\dot{y} < 0$ for $p(x) < \delta$. The region $p(x) < \delta$ contains a strip $x \in [0, \varepsilon]$ for some positive ε. Also, in the region $x \in [0, 1]$, we have that $\dot{x} < 0$ as soon as $y > \frac{\rho x(1-x)}{p(x)}$. Let

$$N = \max_{x \in [\varepsilon, 1]} \frac{\rho x(1-x)}{p(x)}. \tag{2.1}$$

Let us show that there exists a trajectory $(x(t), y(t))$, $t \in (0, T)$ such that $x(0) = 1$, $x(T) = \varepsilon$ and for all t, $y(t) \geq N$. Indeed

$$\frac{dy}{dx} = -\frac{p(x) - \delta}{p(x) - \frac{\rho x(1-x)}{y}}. \tag{2.2}$$

For large y this tends to $-\frac{p(x)-\delta}{p(x)}$ which is bounded on $x \in [\varepsilon, 1]$. Let $(x_1(t), y_1(t))$, $t \in [0, T_1]$ be the lowest such trajectory. Let

$$R = \max_{t \in [0, T_1]} y_1(t). \tag{2.3}$$

From (2.2) it is clear that $\frac{dy}{dx}$ is bounded in the half-strip $x \in [\varepsilon, 1]$, $y > N$. Hence trajectories cannot go to infinity in the positive y direction and they need enter the strip $x \in [0, \varepsilon]$. Once a trajectory has entered this strip, either it remains in this strip with decreasing y or it enters in the strip $[\varepsilon, 1]$ at a height $y < N$. In both cases it is trapped and it stays for ever below the height $y = R$. □

3 Bifurcation of Number of the Singular Points

We give different surfaces in the parameter space which describe the bifurcation of the number of singular points in the first quadrant. There are always two singular points on the x-axis: $(0, 0)$ and $(1, 0)$, but $(1, 0)$ can change multiplicity when singular points enter or exit the first quadrant. In addition, a singular point of multiplicity 2 may appear in the first quadrant and bifurcate into 2 singular points. In the case $\beta \geq 0$ (resp. $\beta < 0$) there is a possibility of up to one singular point (resp. two singular points) in the open first quadrant.

We want to determine the singular points of the system (1.3) apart from those on the x-axis. There is the possibility of up to two singular points in the open first quadrant which are the solutions of $p(x) = \delta$ with $y = \frac{\rho}{\delta}x(1-x)$. We must verify the number of positive solutions of $p(x) = \delta$ such that $\frac{\rho}{\delta}x(1-x) \geq 0$. The number of real solutions of $p(x) = \delta$ is determined by the sign of:

$$\Delta = \delta(\delta\beta^2 - 4\alpha\delta + 4). \tag{3.1}$$

The study of the sign of y is more difficult, but y can only change sign by vanishing or going to infinity. We will show that the latter is excluded when we are in the first quadrant. Hence we will conclude that the number of singular points in the first quadrant can only change in two ways. The first when a singular point passes through the singular point $(1, 0)$. The second when two singular points coalesce and then vanish. We will study both bifurcations.

For the case $\beta \geq 0$ we note that $p'(x) > 0$ for all $x > 0$, therefore $p(x) = \delta$ has at most one positive solution x_0. It is possible that a singular point (x_0, y_0) is not in the first quadrant and, in consequence, has no biological significance. The number of points in the first quadrant is given by the following theorem.

Theorem 3.1 *For all parameter values,* $(0, 0)$ *and* $(1, 0)$ *are singular points of the system* (1.3)*. The number of singular points in the open first quadrant is given in Fig. 3.1.*

The surfaces appearing in Fig. 3.1 are defined below. To help define the surfaces we consider the Jacobian of the system (1.3):

$$A = \begin{bmatrix} \rho - 2\rho x - \frac{xy(\beta x+2)}{(\alpha x^2+\beta x+1)^2} & \frac{-x^2}{\alpha x^2+\beta x+1} \\ \frac{xy(\beta x+2)}{(\alpha x^2+\beta x+1)^2} & -\delta + \frac{x^2}{\alpha x^2+\beta x+1} \end{bmatrix}. \tag{3.2}$$

$\mathcal{S}_1$**:** The Jacobian has a zero eigenvalue at $(1, 0)$ when the parameters are on

$$\mathcal{S}_1 : \qquad \delta = \frac{1}{\alpha + \beta + 1}.$$

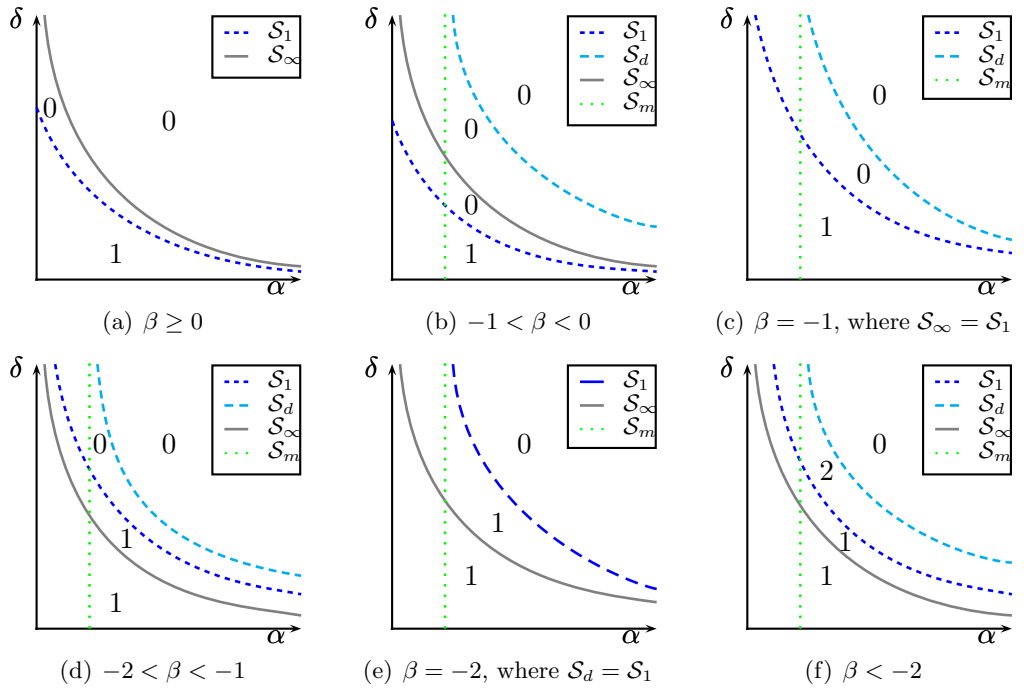

(a) $\beta \geq 0$ (b) $-1 < \beta < 0$ (c) $\beta = -1$, where $\mathcal{S}_\infty = \mathcal{S}_1$

(d) $-2 < \beta < -1$ (e) $\beta = -2$, where $\mathcal{S}_d = \mathcal{S}_1$ (f) $\beta < -2$

Figure 3.1: Surfaces of parameters and number of singular points.

This corresponds to $(1, 0)$ being a saddle-node for $\beta \neq -2$ or a singular point of multiplicity 3 if $\beta = -2$. When crossing $\mathcal{S}_1$ a singular point passes through $(1, 0)$ and changes quadrant. In the case where $\beta > -2$: if $\delta < \frac{1}{\alpha+\beta+1}$ (resp. $\delta > \frac{1}{\alpha+\beta+1}$) then the singular point is in the first (resp. fourth) quadrant, and we have the inverse situation when $\beta < -2$.

$\mathcal{S}_d$: The surface $\mathcal{S}_d$ represents when a singular point in the open first quadrant is of multiplicity 2. The surface has a biological significance when $\beta \leq -2$. We observe that $p(x) = \delta$ if and only if $f(x) = 0$ where

$$f(x) \quad = (\alpha\delta - 1)x^2 + \beta\delta x + \delta. \tag{3.3}$$

The surface $\mathcal{S}_d$ corresponds to the discriminant Δ (see (3.1)) of $f(x)$ being zero. Therefore the surface $\mathcal{S}_d$ is given by

$$\mathcal{S}_d : \qquad \delta = \frac{4}{4\alpha - \beta^2}.$$

We observe that the surface $\mathcal{S}_d$ and $\mathcal{S}_1$ are identical when $\beta = -2$, in which case $(1, 0)$ is a singular point of multiplicity 3.

$\mathcal{S}_m$: The surface $\mathcal{S}_m$ represents the boundary of the parameter region where the model has biological significance in the first quadrant. The model has a biological significance when the generalised Holling function of type III is

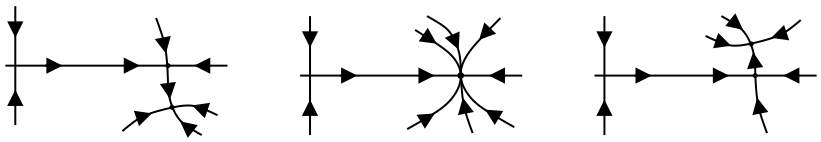

(a) $\beta = -2 + \epsilon$ (b) $\beta = -2$ (c) $\beta = -2 - \epsilon$

Figure 4.1: Behavior of solutions in a neighborhood of the x-axis when the paramenters are on the surface $\mathcal{S}_1$ and in a neighborhood of $\beta = -2$.

well defined (i.e. when the denominator of $p(x)$ does not vanish). The condition is $\beta^2 - 4\alpha < 0$ when $\beta < 0$ and the surface is given by

$$\mathcal{S}_m : \qquad \beta^2 = 4\alpha.$$

$\mathcal{S}_\infty$: This surface represents a singular point which passes to infinity as its x-coordinate becomes infinite. The surface is given by

$$\mathcal{S}_\infty : \qquad \delta = \frac{1}{\alpha}$$

Note that the surfaces $\mathcal{S}_1$ and $\mathcal{S}_\infty$ are identical when $\beta = -1$. In addition we notice that the surface $\mathcal{S}_\infty$ is not relevant for the biological system since it does not change the number of singular points in the first quadrant. This comes from the fact that a singular point can only tend to infinity while it is in the region $y < 0$ and hence it moves from the fourth to the third quadrant.

4 Type of Singular Points

4.1 Statements of Results

Theorem 4.1 *The singular point at the origin is a saddle. The type of* $(1, 0)$ *is:*

- $\delta > \frac{1}{\alpha+\beta+1}$*: an attracting node,*
- $\delta < \frac{1}{\alpha+\beta+1}$*: a saddle,*
- $\delta = \frac{1}{\alpha+\beta+1}$ *and*
  - $\beta \neq -2$*: an attracting saddle-node (see Fig. 4.1),*
  - $\beta = -2$*: an attracting semi-hyperbolic node (see Fig. 4.1).*

The unfolding of the semi-hyperbolic node $(1, 0)$ *of codimension 2 is a cylinder over the bifurcation diagram given in Fig. 4.2.*

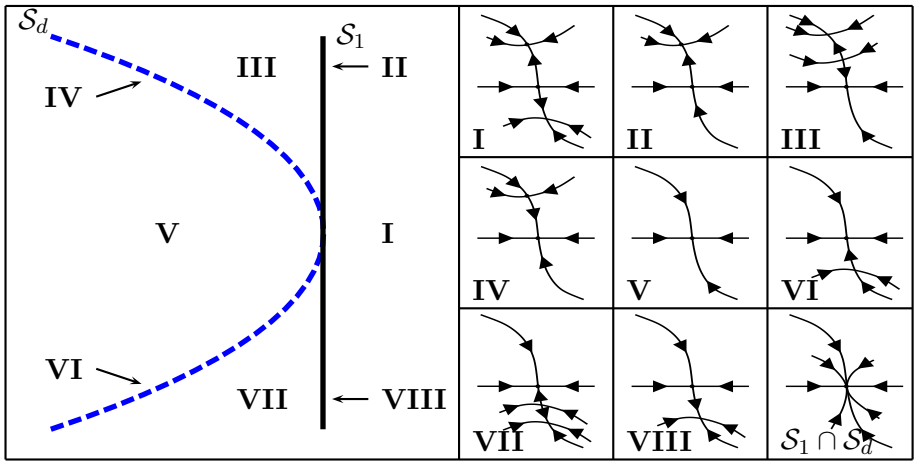

Figure 4.2: Bifurcation diagram of the semi-hyperbolic point $(1, 0)$ of codimension 2.

Theorem 4.2 *If the parameters of the system* (1.3) *are on the surface* $\mathcal{S}_d$, $\beta < -2$ *and* $\beta \neq -4$ *then there is a saddle-node in the open first quadrant. If* $\beta \in (-4, -2)$ *then the saddle-node is attracting. If* $\beta < -4$ *then the saddle-node is repelling.*

Definition 4.3 A singular point is *simple* if the determinant $\det(A_{(x_0,y_0)})$ of the Jacobian $A_{(x_0,y_0)}$ is not zero. A singular point is of *saddle* (resp. *anti-saddle*) type if the determinant, $\det(A_{(x_0,y_0)})$, is negative (resp. positive).

It follows that a singular point of *anti-saddle* type is either a center, a node, a focus, or a weak focus.

Theorem 4.4 *If there exists exactly one simple singular point in the open first quadrant then it is an anti-saddle. If there exists exactly two simple singular points in the open first quadrant then the singular point on the left is an anti-saddle and the singular point on the right is a saddle.*

4.2 Proofs of Results

Proof of Theorem 4.1. The Jacobian A (see (3.2)) evaluated at $(0, 0)$ is

$$A_{(0,0)} = \begin{bmatrix} \rho & 0 \\ 0 & -\delta \end{bmatrix}.$$

It clearly follows that the origin is a saddle since it has eigenvalues ρ and $-\delta$ with eigenvectors $(1, 0)$ and $(0, 1)$, respectively. We observe directly from the system (1.3) that the x and y axes are invariant.

If A is evaluated at $(1, 0)$ we obtain

$$A_{(1,0)} = \begin{bmatrix} -\rho & -\frac{1}{\alpha+\beta+1} \\ 0 & -\delta + \frac{1}{\alpha+\beta+1} \end{bmatrix}.$$

We notice that $-\rho$ is always an eigenvalue and its associated eigenvector is (1,0), hence there is an heteroclinic connection between the singular points, on the x-axis. The second eigenvalue is $-\delta + \frac{1}{\alpha+\beta+1}$, its sign depends on the parameters. If the parameters are 'above' the surface $\mathcal{S}_1$, i.e. $\delta > \frac{1}{\alpha+\beta+1}$, then $(1,0)$ is an attracting node. If the parameters are 'below' the surface $\mathcal{S}_1$, i.e. $\delta < \frac{1}{\alpha+\beta+1}$, then $(1,0)$ is a saddle.

If the parameters are on the surface $\mathcal{S}_1$ (i.e. satisfy the relation $\delta = \frac{1}{\alpha+\beta+1}$), then the second eigenvalue is zero. To determine the type of $(1,0)$, we first localise the system at $(1,0)$ and diagonalise the linear part. We obtain the following system

$$\begin{aligned} \dot{X} &= -\rho X + o(|X,Y|) \\ \dot{Y} &= BY^2 + o(|X,Y|^2) \end{aligned} \tag{4.1}$$

where

$$B = -\frac{2+\beta}{\rho(\alpha+\beta+1)^3}.$$

If a change of coordinates is performed to bring the system onto the center manifold, the term BY^2 does not change. Hence the local behavior of the solutions is determined by B when $B \neq 0$. The singular point $(1,0)$ is an attracting saddle-node when the parameters are on the surface $\mathcal{S}_1$ and $\beta \neq -2$.

The surfaces $\mathcal{S}_d$ and $\mathcal{S}_1$ intersect on $\beta = -2$, in which case $(1,0)$ is of multiplicity 3. Then (4.1) has the following form

$$\begin{aligned} \dot{X} &= -\rho X + o(|X,Y|) \\ \dot{Y} &= CY^3 + XO(|X,Y|^2) + o(|X,Y|^3) \end{aligned}$$

where

$$C = -\frac{1}{\rho(\alpha-1)^4\rho^2}.$$

The term CY^3 is sufficient to determine the local behavior of the solutions since it remains unchanged when reducing the flow on the center manifold. Hence $(1,0)$ is a semi-hyperbolic attracting node since C is always negative. □

Proof of Theorem 4.2. The Jacobian A evaluated at the singular point $(x_0, y_0) = (-\frac{2}{\beta}, -\frac{2\rho(\beta+2)}{\delta\beta^2})$ of multiplicity 2 is

$$A_{(x_0,y_0)} = \begin{bmatrix} \frac{\rho(\beta+4)}{\beta} & \frac{4}{\beta^2-4\alpha} \\ 0 & 0 \end{bmatrix},$$

and its trace is equal to $\frac{\rho(\beta+4)}{\beta}$. Hence (x_0, y_0) is an attracting (resp. repelling) saddle-node for $\beta < -4$ (resp. $\beta > -4$). □

We introduce some relations and a function which will be used both for the proof of Theorem 4.4 and for the study of the Hopf bifurcation. The singular point

(x_0, y_0) is not necessarily on the x-axis if $p(x_0) = \delta$ (see (1.4)), in which case the following two relations are satisfied

$$\mathbf{I}: \qquad \delta = \frac{x_0^2}{\alpha x_0^2 + \beta x_0 + 1}, \tag{4.2}$$

and

$$\mathbf{II}: \qquad y_0 = \frac{\rho}{\delta} x_0 (1 - x_0). \tag{4.3}$$

To determine the type of the singular point we take the determinant of A (Jacobian of the system, see (3.2)) and evaluate it at a singular point not necessarily on the x-axis,

$$\det(A_{(x_0,y_0)}) = \tfrac{x_0^3 y_0(\beta x_0+2)}{(\alpha x_0^2+\beta x_0+1)^3}.$$

It is possible to simplify $\det(A_{(x_0,y_0)})$ by substituting **II** and **I**, yielding

$$\begin{aligned} \det(A_{(x_0,y_0)}) &= -\frac{(-1+x_0)(x_0\beta+2)\rho x_0^2}{(\alpha x_0^2 + x_0\beta + 1)^2} \\ &= -\delta^2(-1+x_0)(x_0\beta+2)\rho \\ &= h(x_0) \end{aligned}$$

for h defined by

$$h(x) = \delta^2(1-x)(x\beta+2)\rho. \tag{4.4}$$

Proof of Theorem 4.4. By continuity the determinant of a singular point cannot change sign without vanishing. There are only two posibilities for $h(x) = 0$, namely $x = 1$ or $x = \frac{-2}{\beta}$. We obtain a surface of parameters where the determinant is zero at a singular point by evaluating $f(x)$ (see (3.3)) for each case. The relation $f(1) = 0$ and $f(\frac{-2}{\beta}) = 0$ are in fact the surfaces $\mathcal{S}_1$ and $\mathcal{S}_d$, respectively. Therefore the sign of the determinant of a singular point in the first quadrant will only change on the bifurcation surfaces $\mathcal{S}_1$ and $\mathcal{S}_d$. Hence the sign of the determinant of the Jacobian at a singular point in the open first quadrant is determined by the local analysis of the bifurcations. As we have studied the bifurcations on $\mathcal{S}_1$ and $\mathcal{S}_d$, this completes the proof of the theorem. □

5 Bogdanov-Takens Bifurcation

Theorem 5.1 *If the parameters are on $\mathcal{S}_d$, $\beta = -4$, $\alpha > 4$ and $\alpha \neq 8$, then there exists a Bogdanov-Takens bifurcation of codimension 2 at a singular point located in the first quadrant: the system localised at the singular point of multiplicity 2 is conjugate to*

$$\begin{aligned} \dot{x}_2 &= y_2 \\ \dot{y}_2 &= x_2^2 + D x_2 y_2 + o(|x_2, y_2|^2) \end{aligned} \tag{5.1}$$

where

$$D \quad = \frac{2\rho(8-\alpha)}{\alpha-4}. \tag{5.2}$$

Theorem 5.2 *Hence the Bogdanov-Takens bifurcaIf the parameters are on $\mathcal{S}_d$ and $(\alpha, \beta) = (8, -4)$ then there exists an attracting Bogdanov-Takens bifurcation of codimension 3 at a singular point located in the first quadrant: the system localised at the singular point of multiplicity 2 is equivalent to*

$$\begin{aligned} X' &= Y \\ Y' &= X^2 + EX^3Y + o(|X, Y|^4) \end{aligned} \tag{5.3}$$

where

$$E \quad = \frac{-1024}{\rho^2}. \tag{5.4}$$

Proof of Theorem 5.1. If the parameters are on the surface $\mathcal{S}_d$ and $\beta = -4$ then the Jacobian evaluated at the singular point $(x_0, y_0) = (-\frac{2}{\beta}, -\frac{2\rho(\beta+2)}{\delta\beta^2})$ of multiplicity 2,

$$A_{(x_0,y_0)} = \begin{bmatrix} 0 & \frac{1}{4-\alpha} \\ 0 & 0 \end{bmatrix},$$

is nilpotent. Therefore it has two zero eigenvalues and we observe that $\frac{1}{4-\alpha} < 0$ since $\beta^2 - 4\alpha < 0$ and $\beta = -4$ which implies $\alpha > 4$ (restriction of the parameters by the surface $\mathcal{S}_m$). This implies that the linear part of the system is non-diagonalisable, hence there is a Bogdanov-Takens bifurcation.

To study the Bogdanov-Takens bifurcation, we want to put the system into the form (5.1). We perform two changes of coordinates. The first step is to localise the singular point (x_0, y_0) to the origin by means of $(x_1, y_1) = (x - x_0, y - y_0)$ and to perform a second changes of coordinates,

$$\begin{aligned} x_2 &= \frac{4\rho}{(\alpha-4)^2}x_1 \\ y_2 &= \frac{4\rho}{(\alpha-4)^2}\left(\frac{1}{4-\alpha}y_1 + \frac{8-\alpha}{4-\alpha}x_1^2 + \frac{16\rho}{4-\alpha}x_1^3 + \frac{16}{(\alpha-4)^2}x_1^2y_1\right. \\ &+ \left.\frac{16(3\alpha-16)\rho}{(\alpha-4)^2}x_1^4 + \frac{-64}{(\alpha-4)^2}x_1^3y_1 + o(|x_1, y_1|^4)\right). \end{aligned}$$

Simplifying we obtain a system of the form (5.1) with D given in (5.2). D is well defined since $\alpha > 4$. The coefficient D can change sign, therefore we continue the analysis of the Bogdanov-Takens bifurcation.

If $D \neq 0$ and there exists an unfolding of (5.1) then we have a system of the form

$$\begin{aligned} \dot{x}_2 &= y_2 \\ \dot{y}_2 &= \mu_1 + \mu_2 y + x_2^2 + Dx_2y_2 + o(|x_2, y_2|^2), \end{aligned}$$

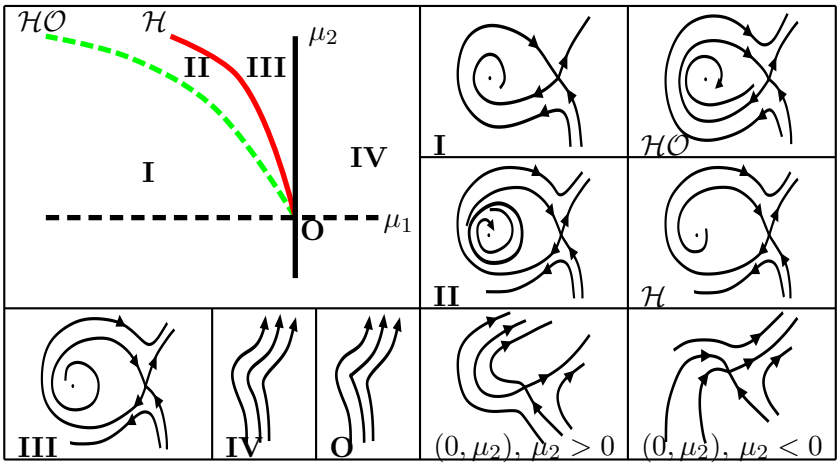

Figure 5.1: Bogdanov-Takens bifurcation diagram when $D > 0$.

and in the case $D > 0$ the system will have the bifurcation diagram given in Fig. 5.1. In the case $D < 0$ the bifurcation diagram can be obtained by applying the transformation $(x_2, y_2, t, \mu_1, \mu_2) \to (x_2, -y_2, -t, \mu_1, -\mu_2)$ to the bifurcation diagram of Fig. 5.1. The Bogdanov-Takens bifurcation is studied in [2, 9, 17]. □

If $\alpha = 8$ then $D = 0$ and we have the following system

$$\begin{aligned}
\dot{x}_2 &= y_2 \\
\dot{y}_2 &= x_2^2 - \frac{16}{\rho}x_2^3 + \frac{64}{\rho^2}x_2^4 \\
&\quad + y_2\left(-\left(\frac{16}{\rho^2} + \frac{192}{\rho}\right)x_2^2 + \left(\frac{256}{\rho^3} + \frac{2048}{\rho^2}\right)x_2^3\right) \\
&\quad + y_2^2\left(-\frac{128}{\rho^2}x_2 + \frac{3072}{\rho^3}x_2^2\right) + o(|x_2, y_2|^4).
\end{aligned} \tag{5.5}$$

We want to bring it to the normal form (5.3), for that purpose we introduce the following result.

Proposition 5.3 *The system*

$$\begin{aligned}
\dot{x} &= y \\
\dot{y} &= x^2 + a_{30}x^3 + a_{40}x^4 + y(a_{21}x^2 + a_{31}x^3) + y^2(a_{12}x + a_{22}x^2) + o(|x, y|^4)
\end{aligned} \tag{5.6}$$

is equivalent to the system

$$\begin{aligned}
X' &= Y \\
Y' &= X^2 + EX^3Y + o(|X, Y|^4)
\end{aligned} \tag{5.7}$$

where

$$E = a_{31} - a_{30}a_{21} \tag{5.8}$$

after changes of coordinates and a rescaling of time.

Proof. The first change of coordinates removes the terms x^2y, xy^2, x^2y^2.

$$\begin{aligned} x &= x_3 + N_1x_3y_3 + N_2x_3^3 + N_3x_3^4 + N_4x_3^3y_3 \\ y &= y_3 + N_1y_3^2 + N_1x_3^3 + 3N_2x_3^2y_3 + a_{30}N_1x_3^4 + 4N_3x_3^3y_3 + 3N_4x_3^2y_3^2 \end{aligned}$$

where $(N_1, N_2, N_3, N_4) = (\frac{a_{21}}{3}, \frac{a_{12}}{6}, \frac{10a_{21}^2+9a_{22}}{108}, \frac{a_{21}a_{12}}{6})$. Using the above change of coordinate we obtain the system

$$\begin{aligned} \dot{x}_3 &= y_3 + o(|x_3, y_3|^4) = h(x_3, y_3) \\ \dot{y}_3 &= k(x_3) + Ex_3^3y_3 + o(|x_3, y_3|^4) \end{aligned}$$

where $k(x) = x^2 + b_{30}x^3 + b_{40}x^4$ and $(b_{30}, b_{40}, E) = (a_{30}, a_{40} - \frac{a_{12}}{6}, a_{31} - a_{30}a_{21})$. We perform a second change of coordinates,

$$\begin{aligned} x_4 &= x_3 \\ y_4 &= h(x_3, y_3) = y_3 + n(x_3, y_3). \end{aligned}$$

with $h(x, y) = o(|x, y|^4)$ which results in the system brings the system to

$$\begin{aligned} \dot{x}_4 &= y_4 + o(|x_4, y_4|^4) \\ \dot{y}_4 &= k(x_4) + Ex_4^3y_4 + o(|x_4, y_4|^4). \end{aligned}$$

For the third change, let $K(x) = \int_0^x k(z)dz$ and

$$\begin{aligned} X &= (3K(x_4))^{\frac{1}{3}} = x_4 + o(|x_4|) \\ Y &= y_4 \end{aligned}$$

be a change of coordinates tangent to the identity. If we perform the change of coordinates we obtain

$$\begin{aligned} \dot{X} &= (3K(x_4))^{-\frac{2}{3}}k(x_4)Y \\ \dot{Y} &= k(x_4) + Ex_4^3Y + o(|x_4, Y|^4). \end{aligned}$$

We then rescale the time by dividing the system by $(3K(x_4))^{-\frac{2}{3}}k(x_4) = 1+O(|x_4|)$ this will not change the orientation nor the qualitative behavior of the solution since the dividing factor is positive in a neighborhood of the bifurcation. With proper substitution we obtain the system (5.7). □

Proof of Theorem 5.2. Using Proposition 5.3 the system (5.5) is equivalent to a system of the form (5.3) where E is given in (5.4). □

The coefficient E is always negative and a system of this form has been studied in [11, 9]. The bifurcation diagram for such a system is known and, if there exists an unfolding, then the unfolding of the system (5.3) is equivalent to

$$\begin{aligned} \dot{x} &= y \\ \dot{y} &= \mu_1 + \mu_2y + \mu_3xy + x^2 - x^3y + o(|x, y|^4). \end{aligned}$$

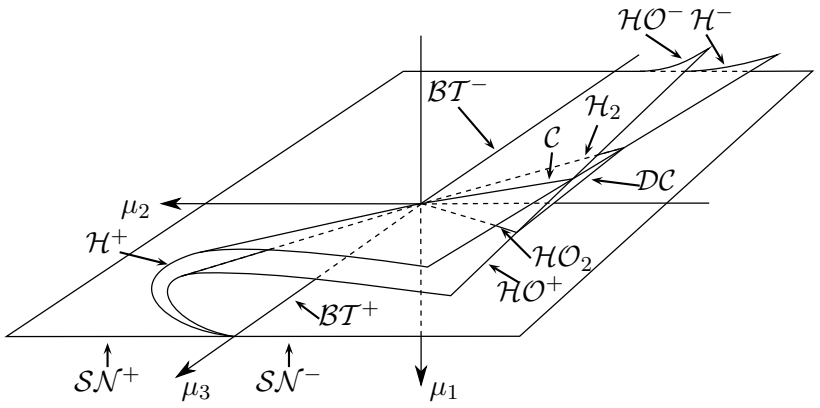

Figure 5.2: Bifurcation diagram for the Bogdanov-Takens singularity of codimension 3.

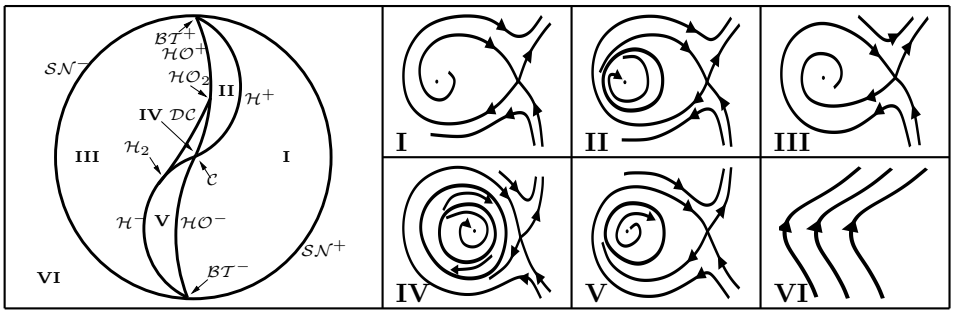

Figure 5.3: Intersection of the bifurcation diagram of a Bogdanov-Takens bifurcation of codimension 3 with a sphere minus a point and generic phase portraits.

We give a bifurcation diagram in Fig. 5.2 and Tab. 5 gives a description of the bifurcation surfaces. The bifurcations $\mathcal{BT}^-$ and $\mathcal{BT}^+$ occur on the μ_3-axis, separated by the Bogdanov-Takens bifurcation of codimension 3.

To visualize the generic regions of the bifurcation diagram we notice that, when $\mu_1 > 0$, there is no singular point, hence the bifurcations are in the half-space where $\mu_1 < 0$. We take a sphere $S_\epsilon = \{(\mu_1, \mu_2, \mu_3) \mid \mu_1^2 + \mu_2^2 + \mu_3^2 = \epsilon^2\}$, which we intersect with the bifurcation diagram of Fig. 5.2 and we then remove a point on the sphere in the region with no singular point. The sphere minus the point can be represented on a plane and the bifurcation diagram appears in Fig. 5.3.

Remark 5.4 Figure 5.2 will be found as an organizing center for our bifurcation diagram. Indeed the role of the parameter μ_2 will be played by $\beta + 4$. Consider cutting the bifurcation diagram of Figure 5.2 with planes $\mu_2 = C$. This will cor-

$\mathcal{H}^+$	repelling Hopf bifurcation
$\mathcal{H}^-$	attracting Hopf bifurcation
$\mathcal{HO}^+$	repelling homoclinic bifurcation
$\mathcal{HO}^-$	attracting homoclinic bifurcation
$\mathcal{H}_2$	Hopf bifurcation of codimension two
$\mathcal{HO}_2$	homoclinic bifurcation of codimension two
$\mathcal{DC}$	double limit cycle
$\mathcal{C}$	intersection of $\mathcal{H}$ and $\mathcal{HO}$
$\mathcal{BT}^+$	Bogdanov-Takens bifurcation with positive xy coefficient
$\mathcal{BT}^-$	Bogdanov-Takens bifurcation with negative xy coefficient
$\mathcal{SN}^+$	repelling saddle-node
$\mathcal{SN}^-$	attracting saddle-node

Table 1:

respond to our drawings in (α, δ) plane for β constant. The Hopf and homoclinic bifurcation curves will be placed exactly as in the slices $\mu_2 = C$ for $C > 0$ (resp. $C = 0$, $C < 0$) when $\beta \in (-4, -3)$ (resp. $\beta = -4$, $\beta \in (-\beta_0, -4)$, with $\beta_0 < -4$).

6 Hopf Bifurcation

In this section we give a full analysis of the Hopf Bifurcation which is summarised in the following theorem.

Theorem 6.1 *The system* (1.3) *has a generic Hopf bifurcation of codimension 1 when* $\beta \geq 0$ *(bifurcation diagram given in Fig. 6.1). It has a generic Hopf bifurcation of codimension 1 (bifurcation diagram given in Fig. 6.2) or 2 (bifurcation diagram given in Fig. 6.3) when* $\beta < 0$. *In all cases it has a complete unfolding.*

The proof of the theorem is spread throughout sections 6.1 to 6.4. In section 6.1 we study some of the necessary conditions for the Hopf bifurcation. In the sections 6.2 and 6.3 the method of Lyapunov coeffficients is used to determine the codimension of the Hopf bifurcation. We then proceed in sections 6.3 and 6.4 to show that the bifurcation has a complete unfolding.

6.1 Necessary Conditions for the Hopf Bifurcation

We deduce two necessary conditions for the Hopf bifurcation to exist. The trace (resp. determinant) of the Jacobian $A_{(x_0,y_0)}$ evaluated at a singular point in the open first quadrant is zero (resp. positive).

The sign of the determinant of the Jacobian has already been studied in Theorem 4.4.

The trace of A (see (3.2)) at a singular point (x_0, y_0) not necesserily on the x-axis vanishes when $\rho - 2\rho x_0 - \frac{x_0 y_0(\beta x_0+2)}{(\alpha x_0^2+\beta x_0+1)^2} = 0$. With the use of relation **I** and

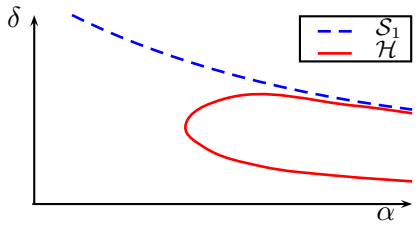

Figure 6.1: Hopf bifurcation diagram when $\beta \geq 0$.

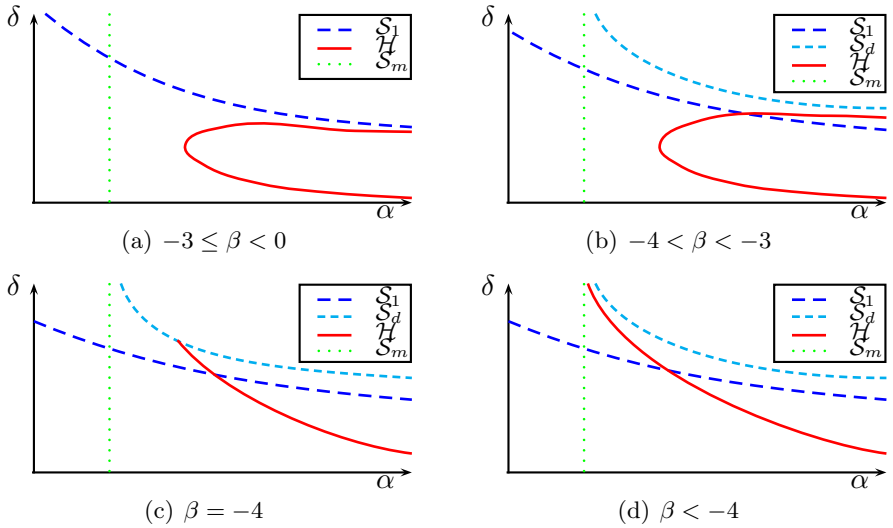

(a) $-3 \leq \beta < 0$ (b) $-4 < \beta < -3$

(c) $\beta = -4$ (d) $\beta < -4$

Figure 6.2: Hopf bifurcation of codimension 1 when $\beta < 0$.

II (see (4.2) and (4.3)) we obtain that the trace of $A_{(x_0,y_0)}$ is zero if and only if $g(x_0) = 0$ where

$$g(x) = -2x^3 + (\beta\delta + 1)x^2 + \delta(2 - \beta)x - 2\delta. \tag{6.1}$$

To obtain a surface in the parameter space which represents the trace of $A_{(x_0,y_0)}$ vanishing for (x_0, y_0) in the first quadrant, we take the resultant of $f(x)$ (see (3.3)) and $g(x)$ with respect to x. This yields $P(\alpha, \beta, \delta) = 0$ where

$$\begin{aligned} P(\alpha,\beta,\delta) &= \frac{\text{resultant}(f(x), g(x), x)}{\delta^2} \\ &= -\alpha(\alpha + \beta + 1)(4\alpha - \beta^2)\delta^3 \\ &+ (\beta^2 - \alpha\beta^2 + \beta^3 + 8\alpha^2)\delta^2 + (-5\alpha + 2\beta)\delta + 1. \end{aligned} \tag{6.2}$$

We note that $P(\alpha, \beta, \delta)$ is a cubic with respect to δ. Hence its discriminant gives information on the number of roots. The discriminant of $P(\alpha, \beta, \delta)$ with respect to δ is

$$Q(\alpha, \beta) = Q_1(\alpha, \beta)Q_2(\alpha, \beta) \tag{6.3}$$

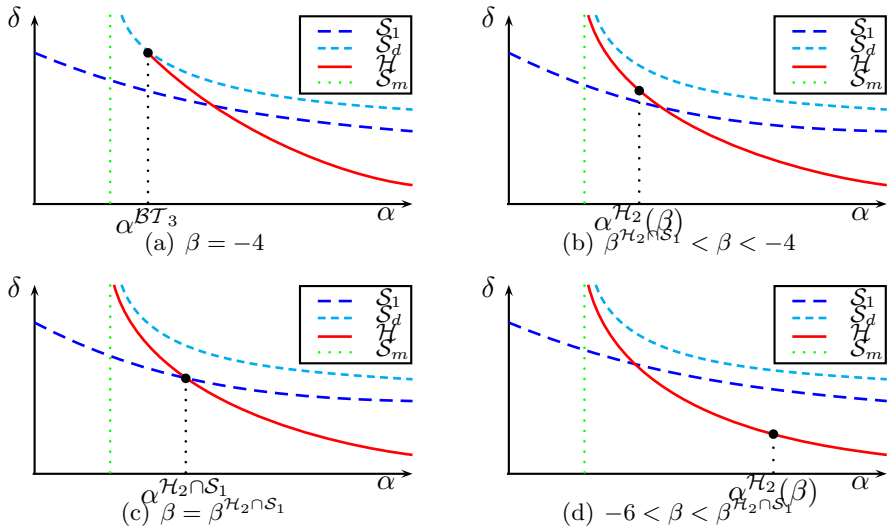

(a) $\beta = -4$ (b) $\beta^{\mathcal{H}_2\cap\mathcal{S}_1} < \beta < -4$

(c) $\beta = \beta^{\mathcal{H}_2\cap\mathcal{S}_1}$ (d) $-6 < \beta < \beta^{\mathcal{H}_2\cap\mathcal{S}_1}$

Figure 6.3: Hopf bifurcation diagram of codimension 2 when $\beta < 0$.

where

$$\begin{aligned} Q_1(\alpha,\beta) &= 4(-\beta^3 + 3\alpha\beta^2 - 3\alpha^2\beta - 27\alpha^2 + \alpha^3) \\ Q_2(\alpha,\beta) &= (-2\alpha + \beta\alpha - \beta^2 - \beta^3)^2. \end{aligned} \tag{6.4}$$

When β is fixed we note that, apart from a double root $\alpha = \alpha^*(\beta)$, $Q_2(\alpha,\beta)$ is always strictly positive, $\alpha^*(\beta)$ is positive if and only if $\beta \in \mathbb{R}\backslash[-2,2]$.

We analyse $Q_1(\alpha,\beta)$ and, since it is cubic in α, we take its discriminant with respect to α which is equal to $-19683\beta^2(\beta+4)$. Hence if $\beta > -4$, (resp. $\beta = -4$, $\beta < -4$) is fixed, then $Q_1(\alpha,\beta) = 0$ has three roots, (resp. one root of multiplicity 2, one root). For $\beta < 0$ there is always an even number of positive roots of $Q_1(\alpha,\beta) = 0$. They are denoted α_1^{**} and α_2^{**} when they exist. When $\beta > 0$, $Q_1(\alpha,\beta)$ has exactly one positive root which is denoted α^{**}.

Proposition 6.2 *If* $\beta_0 = \frac{3\pm\sqrt{13}}{2}$, -2, -4 *then* $Q_1(\alpha,\beta_0) = 0$ *and* $Q_2(\alpha,\beta_0) = 0$ *have a common root.*

Proof. The proof is trivial since the root of $Q_2(\alpha,\beta)$ is explicitly known. □

Proposition 6.3 *For* β *fixed, the graph of the function* $Q(\alpha,\beta)$ *and the algebraic curve* $P(\alpha,\beta,\delta) = 0$ *are given (qualitatively) for generic or bifurcation values of* β *in Fig. 6.5, 6.6, 6.7, 6.8, 6.9, 6.10, 6.11, 6.12, 6.13, 6.14, 6.15.*

Proof. The proof is lenghty but relatively straightforward and consists of a study of $Q(\alpha,\beta)$ and $P(\alpha,\beta,\delta) = 0$ with algebraic tools. In particular a solution branch of $P(\alpha,\beta,\delta) = 0$ tends to infinity with respect to δ for

$$\alpha^\infty = -1 - \beta.$$

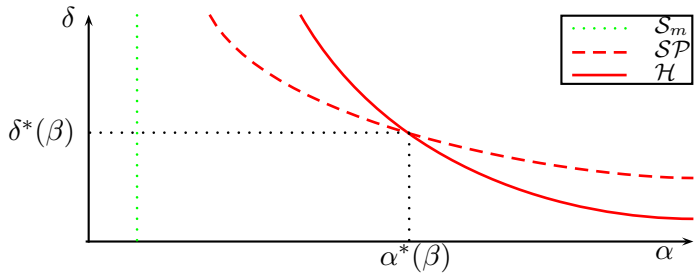

Figure 6.4: Diagram of the curves $\mathcal{SP}$ and $\mathcal{H}$ for $\beta < -4$.

Full details appear in [21]. □

Not all solution branches given above satisfy the necessary condition for the Hopf bifurcation. For example one branch represents a singular point that is not in the first quadrant, while another branch represents a trace zero saddle in the open first quadrant.

Proposition 6.4 *Among the solution branches of $P(\alpha, \beta, \delta) = 0$, only the ones in Fig. 6.1 for $\beta \geq 0$ and in Fig. 6.2 for $\beta < 0$ satisfy the necessary conditions for the Hopf bifurcation.*

Proof. We eliminate the solution branches of $P(\alpha, \beta, \delta) = 0$ which either do not represent a singular point (x_0, y_0) in the open first quadrant, or are attached to a singular point with zero trace at which the determinant of the Jacobian $A_{(x_0,y_0)}$ is negative. In the case $\beta \geq 0$ a branch is easily discarded as part of it is located in a region where the system has no singular point in the open first quadrant. The same reasoning can be applied in the case $\beta \in (-4, 0)$ and the upper left solution branch is discarded. In the case $\beta < -4$, the branch which intersects the valid Hopf solution branch, $\mathcal{H}$, is discarded since it represents a trace zero saddle, $\mathcal{SP}$, see Fig. 6.4. However this branch will be of interest in section 8.4 where we consider the homoclinic bifurcation of codimension 2, $\mathcal{HO}_2$. In the case $\beta < 0$ the lowest solution branch (the one closest to the α-axis) represents a singular point not in the first quadrant, hence it is discarded. Full details appear in [21], [8]. □

6.2 Hopf Bifurcation of Codimension 2

We study the Hopf bifurcation with the method of Lyapunov constants [3, 7, 6, 16]. We first localise the system at a singular point (x_0, y_0) in the open first quadrant. We then rescale the time by dividing the system by $p(x_1 + x_0)$ (see (1.4)). Since $p(x) > 0$ for all $x > 0$, neither the orientation of trajectories, nor the number of periodic solutions will change. The system has the form

$$x_1' = h(x_1) - y_1 \tag{6.5}$$

$$y_1' = (y_1 + y_0)\left(\frac{-\delta}{p(x_1 + x_0)} + 1\right) \tag{6.6}$$

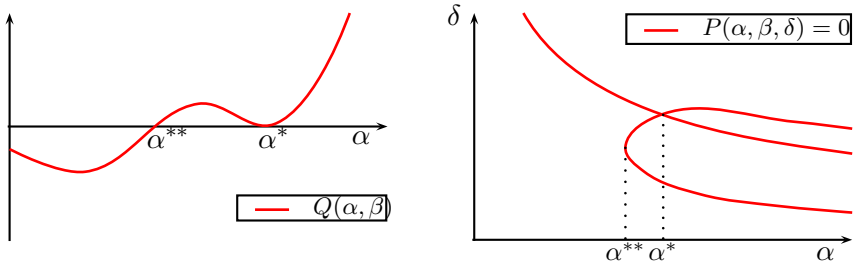

Figure 6.5: $Q(\alpha,\beta)$ and $P(\alpha,\beta,\delta)=0$ when $\beta > \frac{3+\sqrt{13}}{2}$ is fixed.

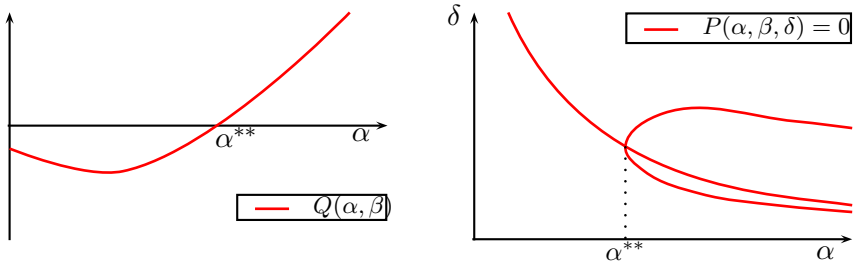

Figure 6.6: $Q(\alpha,\beta)$ and $P(\alpha,\beta,\delta)=0$ when $\beta = \frac{3+\sqrt{13}}{2}$.

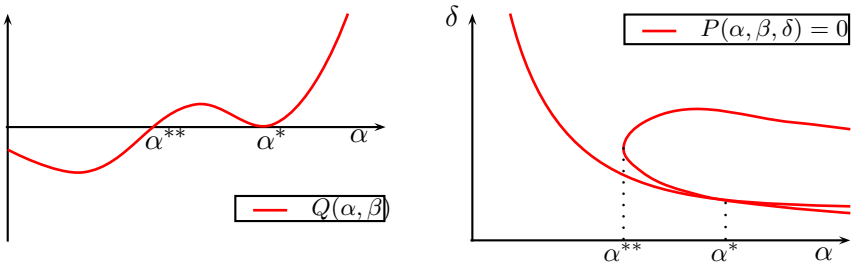

Figure 6.7: $Q(\alpha,\beta)$ and $P(\alpha,\beta,\delta)=0$ when $2 < \beta < \frac{3+\sqrt{13}}{2}$ is fixed.

where

$$h(x) \quad = \quad \frac{\rho(-\alpha(x+x_0)^3+(\alpha-\beta)(x+x_0)^2+(\beta-1)(x+x_0)+1)}{x+x_0} - y_0.$$

We proceed with a second change of coordinates $(x_2,y_2)=(x_1,y_1-h(x_1))$ and we obtain a system of the form

$$\begin{aligned} x_2' &= -y_2 \\ y_2' &= (h(x_2)+y_0)\left(\frac{-\delta}{p(x_2+x_0)}+1\right)+y_2\left(\frac{dh(x_2)}{dx_2}+1-\frac{\delta}{p(x_2+x_0)}\right) \\ &= \sum_{i=1}^{5} a_i(\lambda)x_2^i + y_2\left(\sum_{i=0}^{4} b_i(\lambda)x_2^i + o(|x_2|^4)\right) + o(|x_2|^5). \end{aligned} \tag{6.7}$$

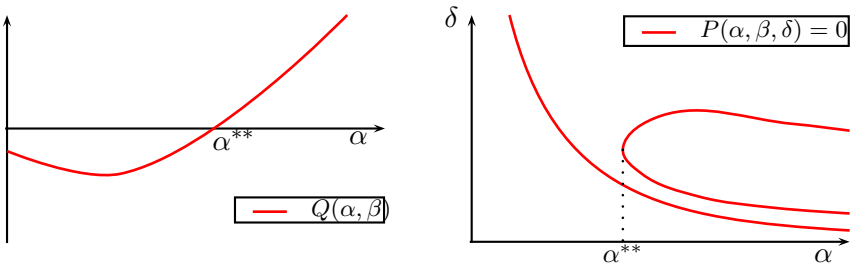

Figure 6.8: $Q(\alpha,\beta)$ and $P(\alpha,\beta,\delta)=0$ when $0\leq\beta\leq 2$ is fixed.

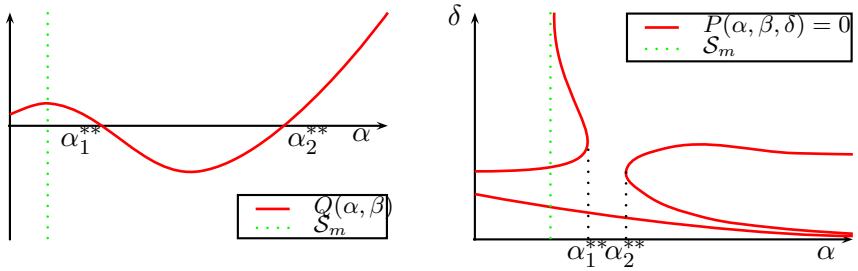

Figure 6.9: $Q(\alpha,\beta)$ and $P(\alpha,\beta,\delta)=0$ when $-1<\beta<0$ is fixed.

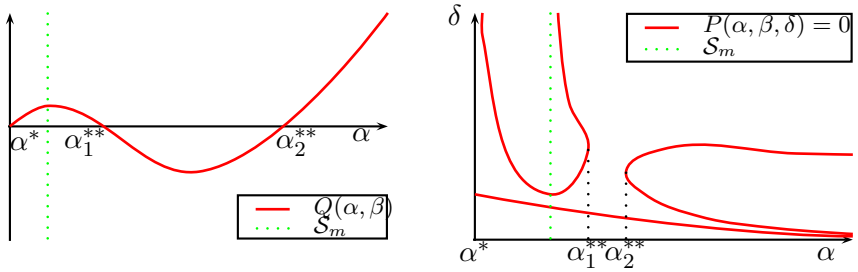

Figure 6.10: $Q(\alpha,\beta)$ and $P(\alpha,\beta,\delta)=0$ when $\beta=-1$.

The method of Lyapunov constants to study the Hopf bifurcation consists of looking for a Lyapunov function for the system. The method is usually applied to a system of the form

$$\begin{aligned}\dot{X}&=c(\lambda)X-Y+G_1(X,Y,\lambda)\\ \dot{Y}&=X+d(\lambda)Y+G_2(X,Y,\lambda)\end{aligned}\tag{6.8}$$

where c,d,G_1,G_2 are smooth functions with $G_i(X,Y)=o(|X,Y|)$ and, either $c\equiv 0$ or $c\equiv d$ and λ a multi-parameter.

Proposition 6.5 *Consider a family of Liénard vector fields* (6.7) *with* λ *a multi-parameter, to which we apply the change of coordinates*

$$\begin{bmatrix}x_2\\ y_2\end{bmatrix}=\begin{bmatrix}1 & 0\\ \frac{-b_0(\lambda)}{2} & \frac{\sqrt{-b_0(\lambda)^2+4a_1(\lambda)}}{2}\end{bmatrix}\begin{bmatrix}X\\ Y\end{bmatrix}.\tag{6.9}$$

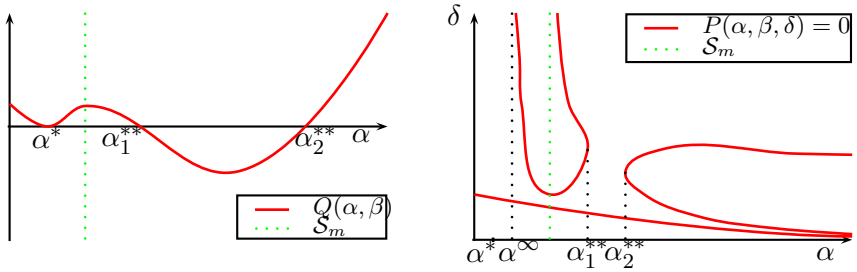

Figure 6.11: $Q(\alpha,\beta)$ and $P(\alpha,\beta,\delta)=0$ when $-2<\beta<-1$ is fixed.

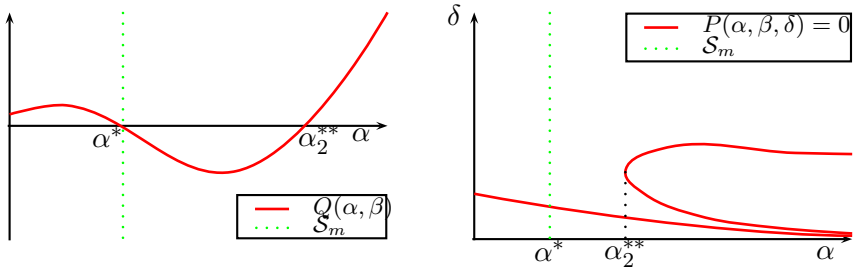

Figure 6.12: $Q(\alpha,\beta)$ and $P(\alpha,\beta,\delta)=0$ when $\beta=-2$.

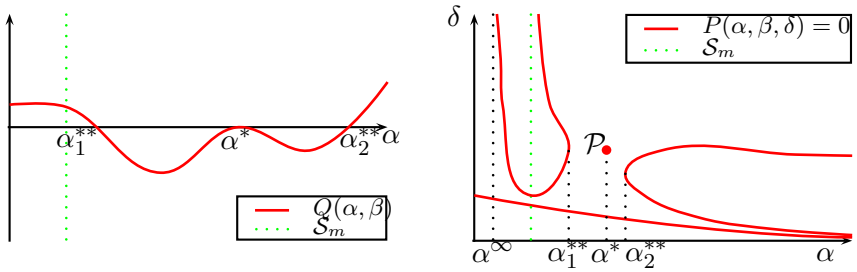

Figure 6.13: $Q(\alpha,\beta)$ and $P(\alpha,\beta,\delta)=0$ when $-4<\beta<-2$ is fixed.

Then there exists a polynomial F_λ,

$$F_\lambda(X,Y)=\frac{1}{2}(X^2+Y^2)+\sum_{j=3}^{6}F_j(X,Y,\lambda),$$

with F_j *a homogeneous polynomial of degree* j *with respect to* X *and* Y. *Then there exists* $L_0(\lambda)$ *such that*

$$\dot{F}_\lambda=L_0(\lambda)(X^2+Y^2)+o(|X,Y|^2),$$

and for all values of λ *such that* $L_0(\lambda)=0$, *there exist* $L_1(\lambda)$ *and* $L_2(\lambda)$ *such that*

$$\dot{F}_\lambda=L_1(\lambda)(X^2+Y^2)^2+L_2(\lambda)(X^2+Y^2)^3+o(|X,Y|^6).$$

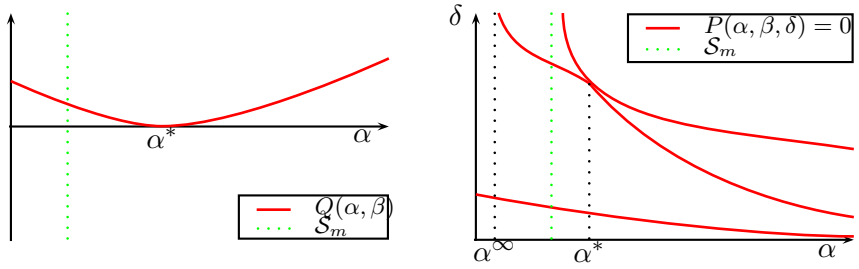

Figure 6.14: $Q(\alpha,\beta)$ and $P(\alpha,\beta,\delta)=0$ when $\beta=-4$.

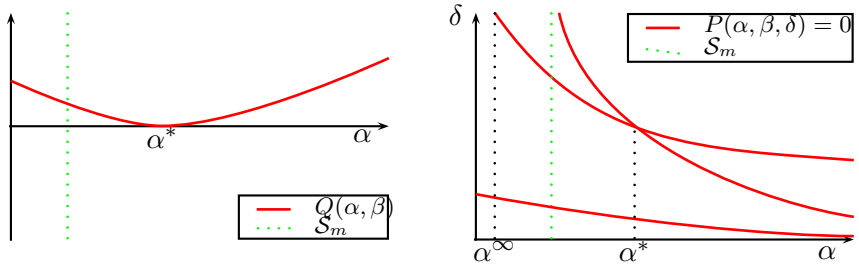

Figure 6.15: $Q(\alpha,\beta)$ and $P(\alpha,\beta,\delta)=0$ when $\beta<-4$ is fixed.

The Lyapunov constants are

$$\begin{aligned} L_0(\lambda) &= \frac{b_0(\lambda)}{2}, \\ L_1(\lambda)\Big|_{L_0=0} &= \frac{b_2(\lambda)a_1(\lambda)-b_1(\lambda)a_2(\lambda)}{8a_1(\lambda)}, \\ L_2(\lambda)\Big|_{L_0=0} &= \frac{1}{192a_1(\lambda)^3}(L_2^{(1)}(\lambda)(b_2(\lambda)a_1(\lambda)-b_1(\lambda)a_2(\lambda))+L_2^{(2)}(\lambda)) \end{aligned} \tag{6.10}$$

where

$$\begin{aligned} L_2^{(1)}(\lambda) &= -21a_3(\lambda)a_1(\lambda)+b_1(\lambda)^2a_1(\lambda)-10a_2(\lambda)^2 \\ L_2^{(2)}(\lambda) &= 12a_1(\lambda)^3b_4(\lambda)-20a_1(\lambda)^2b_3(\lambda)a_2(\lambda) \\ &\quad -12a_1(\lambda)^2b_1(\lambda)a_4(\lambda)+20a_2(\lambda)b_1(\lambda)a_3(\lambda)a_1(\lambda). \end{aligned} \tag{6.11}$$

In addition, L_0, L_1, L_2 are smooth with respect to λ.

Proof. The Lyapunov method guarantees the existence and differentiability of the Lyapunov constants of a system of the form (6.8) shown in [6]. After the change of coordinates given by (6.9) is applied to the system (6.7) we determine the Lyapunov constants. This is an algebraic procedure, therefore it is possible to program it with a symbolic manipulation program. The program used in this case was `MAPLE`. The calculations have been made independently by two authors. □

6.3 Analysis of the Lyapunov Constants

With the analysis of the Lyapunov constants we determine the codimension of the Hopf Bifurcation depending on the parameters. We proceed with the L_0 Lyapunov constant (see (6.10)), once the coefficient b_0 is substituted, L_0 depends on $\alpha, \beta, \delta, \rho, x_0, y_0$. The use of two successive substitutions: substituting y_0 with the relation **II** (see (4.3)), substituting δ with the relation **I** (see (4.2)), removes the dependence on y_0 and δ. Hence, we obtain

$$L_0 = \frac{-(1 + (\beta - \alpha)x_0^2 + 2\alpha x_0^3)\rho}{2x_0^2}. \tag{6.12}$$

As expected it follows that $L_0 = 0$ if and only if the trace of the Jacobian $A_{(x_0,y_0)}$ is zero, which we had shown to be equivalent to $g(x) = 0$ (see (6.1)). The locus in the parameter space where $L_0 = 0$ has already been studied in the analysis of $P(\alpha, \beta, \delta) = 0$.

We continue with the analysis of the first Lyapunov constant L_1 under the hypothesis $L_0 = 0$. Hence $g(x_0) = 0$ (see (6.1)), and we can substitute δ with the relation **I** and isolate α from the factor of the numerator that can vanish in the open first quadrant. We obtain

$$\textbf{III}: \qquad \alpha = \frac{1 + \beta x_0^2}{x_0^2(1 - 2x_0)}. \tag{6.13}$$

The constant L_1 (see (6.10)) depends on $\alpha, \beta, \delta, \rho, x_0, y_0$. The substitution of y_0 with the relation **II** (see (4.3)), and of δ with the relation **I** (see (4.2)) and α with the relation **III**, removes the dependence on y_0, δ and α. Hence, this yields

$$L_1 = \frac{(2x_0^3\beta^2 + (6x_0^2 + 1)\beta + 6)\rho}{8x_0^3(\beta x_0 + 2)(2x_0 - 1)}. \tag{6.14}$$

The following Lemma will be useful for the analysis of L_1 and L_2.

Lemma 6.6 *For $\beta \geq 0$ (resp. $\beta < 0$), if the system (1.3) has a Hopf bifurcation at a point (x_0, y_0), then necessarily $x_0 < \frac{1}{2}$ (resp. $x_0 \neq \frac{1}{2}$).*

Proof. If we suppose $x_0 \geq \frac{1}{2}$ then it implies that, if the numerator of L_0 is zero and α positive, then β is negative. In the case $\beta < 0$, if $x_0 = \frac{1}{2}$ and the Jacobian trace is zero, then $\beta = -4$. It is then the case of the Bogdanov-Takens bifurcation. □

Proposition 6.7 *If $\beta \geq 0$, the Hopf bifurcation is of codimension 1 and the sign of the first Lyapunov constant, L_1, is negative.*

Proof. We observe that the numerator of L_1 (see (6.14)) is always positive which implies that the Hopf bifurcation is at most of codimension 1. By Lemma 6.6 the denominator is negative. Hence L_1 is negative. □

The next proposition explores the possibility of having L_0 and L_1 vanishing.

Proposition 6.8 *If $\beta < 0$, $L_0(\lambda) = 0$ and α is equal to*

$$\alpha^{\mathcal{H}_2}(\beta) = \frac{\beta^2}{\beta + 6} \tag{6.15}$$

then $L_1(\lambda) = 0$. Moreover, if $\beta \in (-6, -4)$ and $\alpha = \alpha^{\mathcal{H}_2}(\beta)$ then there exists λ such that for $\lambda = (\alpha^{\mathcal{H}_2}(\beta), \beta, \delta^{\mathcal{H}_2}(\beta), \rho)$ the system has a Hopf bifurcation of codimension at least 2. See Fig. 6.3.

Proof. It is sufficient to determine when the numerator of L_0 and L_1 have a root in common. We take the resultant of the numerator of L_0 and L_1 with respect to x_0,

$$\text{resultant}(\text{num}(L_0), \text{num}(L_1), x_0) = -2(\beta^2 - \alpha\beta - 6\alpha)^3(\beta + 4)\rho^6.$$

If $L_0(\lambda) = 0$ and α is equal to $\frac{\beta^2}{\beta+6}$ then $L_1(\lambda) = 0$. The case $\beta = -4$ is not a possibility since it is the Bogdanov-Takens bifurcation of codimension 3. □

The above proposition indicates that there exists values of the parameters such that L_0 and L_1 are zero simultaneously. A corollary which follows directly is that the maximum codimension of the Hopf bifurcation is at least 2. We analyse the second Lyapunov constant L_2 under the condition $L_0 = L_1 = 0$, it suffices to analyse $L_2^{(2)}$ (see (6.10)). Using the same simplifications as for L_1 and using that $L_1 = 0$ we get,

$$\begin{aligned} L_2^{(2)} = &\frac{((5x_0^2 - x_0)\beta^2 + (76x_0^2 + \frac{17}{2} - \frac{47}{2}x_0 - 85x_0^3 - 12x_0^5 + 50x_0^4)\beta}{48x_0^5(x_0 - 1)^3(\beta x_0 + 2)^2(2x_0 - 1)} \\ &+ \frac{39 - 57x_0 + 42x_0^2 - 12x_0^3)\rho}{48x_0^5(x_0 - 1)^3(\beta x_0 + 2)^2(2x_0 - 1)}. \end{aligned} \tag{6.16}$$

The next proposition yields that the codimension of the Hopf bifurcation is at most 2.

Proposition 6.9 *The Lyapunov constants L_0, L_1 and L_2 never vanish simultaneously for a singular point in the first quadrant. Moreover the second Lyapunov constant, L_2, is negative when $L_1 = L_0 = 0$.*

Proof. Under the hypothesis $L_0 = 0$ it is sufficient to take the resultant of the numerator of L_1 and L_2 with respect to β,

$$\text{resultant}(\text{num}(L_1), \text{num}(L_2), \beta) = -48x_0(1 + 2x_0 + 12x_0^2)(2x_0 - 1)^2(x_0 - 1)^7\rho^4.$$

Since we only consider a singular point in the open first quadrant then the only possibility of a root in common is $x_0 = \frac{1}{2}$. This is excluded by Lemma 6.6. Therefore L_1 and L_2 never vanish simultaneously.
Secondly, it remains to show that L_2 is negative. Since L_1 and L_2 are not zero simultaneously, L_2 does not change sign when $L_1 = 0$ (by the intermediate value theorem). If $\beta_0 = -\frac{9}{2} \in (-6, -4)$ then for $\alpha = \alpha^{\mathcal{H}_2}(\beta)$ and $x_0 = \frac{1}{3}$ we have $L_0 = L_1 = 0$. If we evaluate $L_2^{(2)}$ at $(x_0, \alpha, \beta) = (\frac{1}{3}, \alpha^{\mathcal{H}_2}\left(-\frac{9}{2}\right), -\frac{9}{2})$, we obtain $L_2^{(2)} = -\frac{2187}{16}\rho$. Therefore L_2 is negative when $L_1 = L_0 = 0$. □

6.4 Submersion of the Lyapunov Constants

We show that all Hopf Bifurcations have a complete unfolding by showing that L_0 and (L_0, L_1) are submersions with respect to the parameters α and δ. For the proof we will need:

$$\frac{\partial x_0(\alpha,\delta)}{\partial \alpha} = -\frac{x_0(\alpha,\delta)^2\delta}{2x_0(\alpha,\delta)\alpha\delta - 2x_0(\alpha,\delta) + \delta\beta} \tag{6.17}$$

and

$$\frac{\partial x_0(\alpha,\delta)}{\partial \delta} = -\frac{x_0(\alpha,\delta)^2\alpha + \beta x_0(\alpha,\delta) + 1}{2x_0(\alpha,\delta)\alpha\delta - 2x_0(\alpha,\delta) + \delta\beta} \tag{6.18}$$

which are obtained by differentiating **I** (see (4.2)) with respect to α and δ, respectively.

Proposition 6.10 *The map $\lambda = (\alpha, \beta, \delta, \rho) \mapsto L_0$ is a submersion with respect to α and δ when $L_0(\lambda) = 0$.*

Proof. It suffices to show that $\frac{\partial L_0}{\partial \alpha}$ and $\frac{\partial L_0}{\partial \delta}$ never vanish simultaneously. Using (6.17), (6.18) and substituting α by the relation **III** (see (6.13)) we obtain

$$\begin{aligned}
\frac{\partial L_0}{\partial \alpha} &= -\frac{(2x_0^3\beta + (8-4\beta)x_0^2 + (\beta-14)x_0 + 4)\rho}{2(\beta x_0 + 2)(2x_0 - 1)} \\
\frac{\partial L_0}{\partial \delta} &= \frac{(x_0-1)^2(\beta x_0 + 2)(x_0^3\beta + 3x_0 - 1)\rho}{x_0^4(2x_0-1)^3}.
\end{aligned}$$

We must verify that $\left[\frac{\partial L_0}{\partial \alpha}(\lambda) \quad \frac{\partial L_0}{\partial \delta}(\lambda)\right]$ has rank 1 for all λ such that $L_0(\lambda) = 0$. The resultant of the numerators of $\frac{\partial L_0}{\partial \alpha}$ and $\frac{\partial L_0}{\partial \delta}$ with respect to β,

$$\text{resultant}\left(\text{num}\left(\frac{\partial L_0}{\partial \delta}\right), \text{num}\left(\frac{\partial L_0}{\partial \alpha}\right), \beta\right) = 2x_0^2(x_0-1)^4(2x_0-1)^4\rho^3,$$

does not vanish since $x_0 \neq 0, \frac{1}{2}, 1$, using Lemma 6.6. □

Proposition 6.11 *The map $\lambda \mapsto (L_0(\lambda), L_1(\lambda))$ is a submersion with respect to α and δ when $L_0 = L_1 = 0$.*

Proof. We want to show that the two vectors $V_i = \left(\frac{\partial L_i}{\partial \alpha}, \frac{\partial L_i}{\partial \delta}\right)$ for $i = 0, 1$, are linearly independent at all points in the parameter space λ_0 where $L_0 = L_1 = 0$. We use the following idea coming from Lemma 6 in [6]: for fixed β_0, let (α_0, δ_0) be a point where $L_0 = L_1 = 0$. Proposition 6.10 ensures that $L_0 = 0$ is a smooth curve near (α_0, δ_0) by the implicit function theorem and that V_0 is normal to $L_0 = 0$. We now restrict L_1 to $L_0(\alpha, \delta) = 0$ and we show that this map is a submersion with respect to δ when $L_0 = L_1 = 0$. This guarantees that V_1 is linearly independent from V_0.

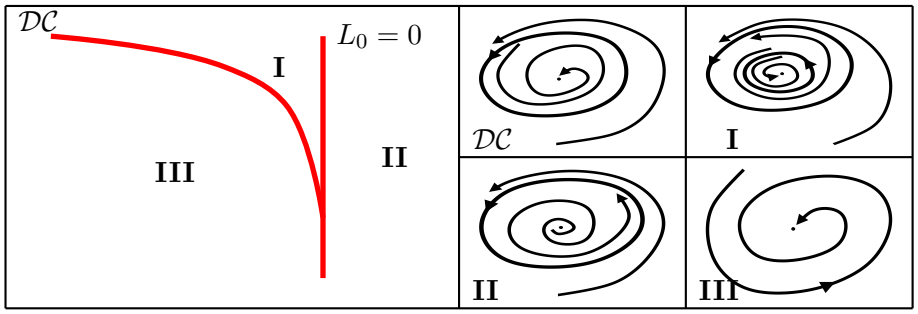

Figure 6.16: Bifurcation diagram of the Hopf bifurcation of codimension 2.

We use the relation **III** (see (6.13)) to simplify L_1 and calculate $\frac{\partial L_1}{\partial \delta}$. After substituting $\frac{\partial x_0(\delta)}{\partial \delta}$ by the relation (6.18), we obtain

$$\begin{aligned}\frac{\partial L_1}{\partial \delta} &= \frac{-1}{4(2x_0-1)^4(2+\beta x_0)x_0^5}[(4x_0-1)x_0^4\beta^3 + (22x_0^3 - 6x_0^2 + 5x_0 - 2)x_0\beta^2 \\ &+ (-3 + 24x_0^3 - 4x_0 + 24x_0^2)\beta + 48x_0 - 18](x_0-1)^2\rho.\end{aligned}$$

L_1 and $\frac{\partial L_1}{\partial \delta}$ do not vanish simultaneously as

$$\text{resultant}\left(\text{num}\left(\frac{\partial L_1}{\partial \delta}\right), \text{num}(L_1), \beta\right) = 216x_0^6(2x_0-1)^4(x_0-1)^6\rho^5$$

does not vanish since $x_0 \neq 0, \frac{1}{2}, 1$ using Lemma 6.6. □

We prove the main theorem of this section.

Proof of Theorem 6.1. If $\beta \geq 0$ there is a Hopf bifurcation of codimension 1. The bifurcation is called *super-critical*: the singular point is stable and, when a limit cycle appears from the singular point, then the singular point becomes unstable and the limit cycle is stable. This follows from the Propositions 6.4, 6.5, 6.7, 6.10 and the fact that the sign of L_1 is negative when $L_0 = 0$.

If $\beta < 0$ there is a Hopf bifurcation of codimension 1 or 2. In the case of the codimension 2, the bifurcation will have the bifurcation diagram given in Fig. 6.16. This follows from the Propositions 6.4, 6.5, 6.8, 6.9, 6.11 and the fact that the sign of L_2 is negative when $L_0 = L_1 = 0$. □

7 Bifurcation Diagram

In this section we conjecture the global topological bifurcation diagram based on the local study of the singular points. In particular we use the local bifurcation diagram near the Bogdanov-Takens bifurcations of codimension 2 and 3 which yields bifurcation surfaces of the homoclinic orbit, $\mathcal{HO}$, and the double limit cycle,

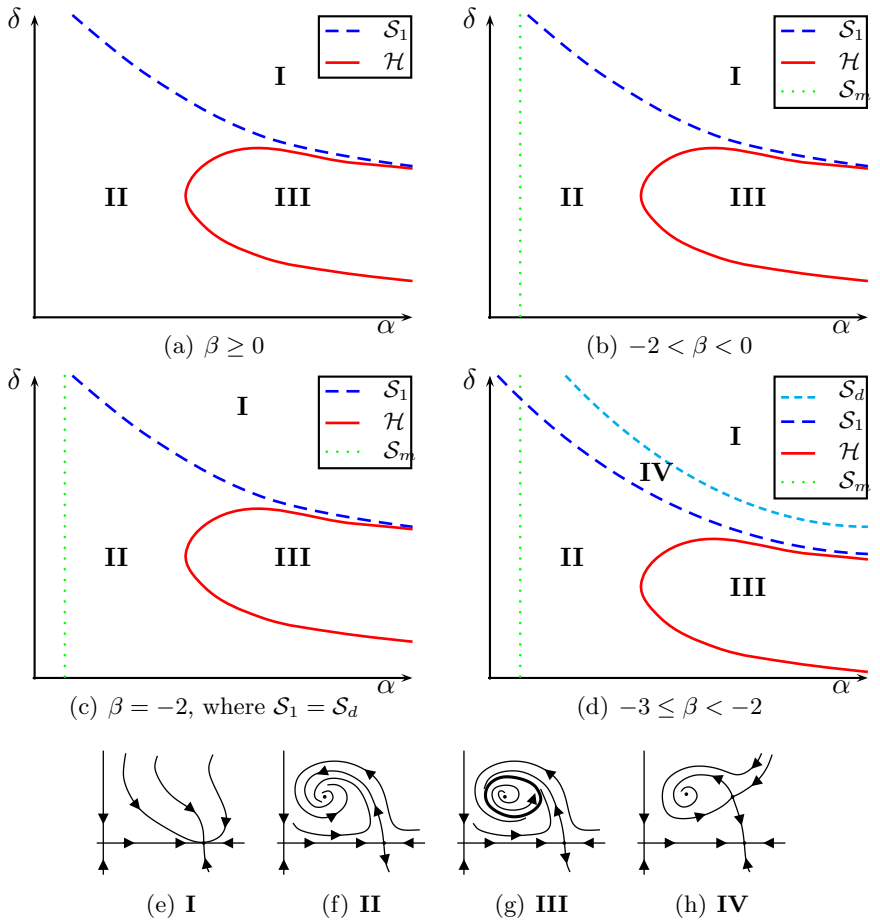

Figure 7.1: Bifurcation diagram and phase portraits for generic regions of parameters.

$\mathcal{DC}$, for β close to -4 (see Remark 5.4). Essentially we conjecture the global extension of these surfaces for other values of β. For the bifurcation diagram we do not consider the parameter ρ since we have shown that it does not have a role in the bifurcation of singular points. We want to represent the bifurcation diagram in the 3-parameter space (α, β, δ). This is accomplished by taking slices with β fixed, where we give the bifurcation diagram in the (α, δ) plane. The values of β for the different slices are either part of a generic interval or bifurcation values. The bifurcation values are those which produce a topological change of the bifurcation diagram in the (α, δ) plane.

For each slice of the bifurcation diagram we identify the open regions in the parameter space: $\mathbf{I}, \mathbf{II}, \mathbf{III}, \ldots$, for each region we give a qualitative phase portrait.

For the case $\beta \geq -3$ (see Fig. 1(a), 1(b), 1(c), 1(d)) there is no intersection between the Hopf bifurcation, $\mathcal{H}$, and the surface $\mathcal{S}_1$. This follows from the result that the intersection between the two surfaces has α-coordinate given by $\alpha^{\mathcal{H}\cap\mathcal{S}_1}(\beta) = \frac{(\beta+1)(\beta^2+3\beta+1)}{\beta+3}$. Hence $\mathcal{H}$ is always located below $\mathcal{S}_1$ or $\mathcal{S}_d$, yield-

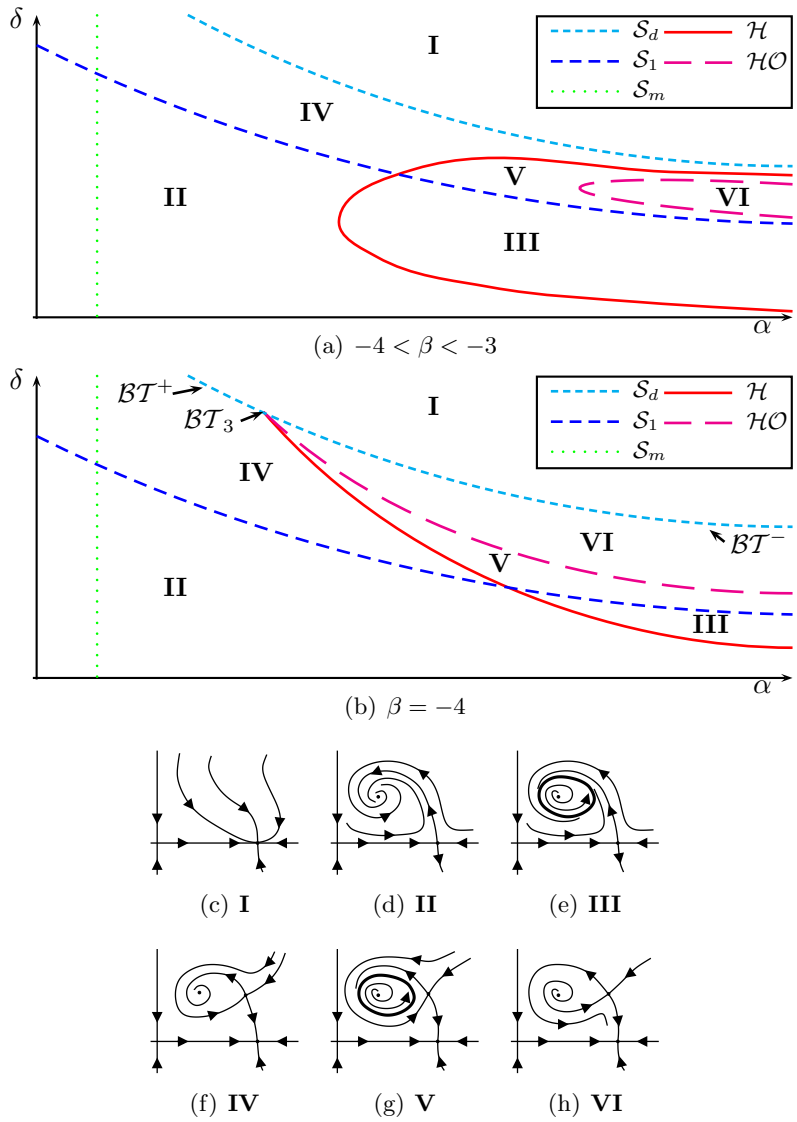

Figure 7.2: Bifurcation diagram and phase portraits for generic regions of parameters.

ing that $\mathcal{H}$ tends to the α-axis as α tends to infinity. Also, we conjecture for $\beta \in [-3, -2)$ (see Fig. 1(d)) that there is no homoclinic orbit, nor any limit cycle, when there are two singular points in the open first quadrant.

In the case $\beta < -3$ (see Fig. 2(a), 2(b), 3(a), 3(b), 4(a), 4(b)) there is an intersection between $\mathcal{H}$ and $\mathcal{S}_1$, hence a limit cycle may exist when there are two singular points in the open first quadrant. In addition, from the unfolding of the Bogdanov-Takens bifurcation of codimension 2 and 3, we know that there is a curve of homoclinic bifurcation for fixed β near -4. We do not know at which value of β such bifurcation curves starts to exist. Near $(\alpha, \beta, \delta) = (8, -4, \frac{1}{4})$ the

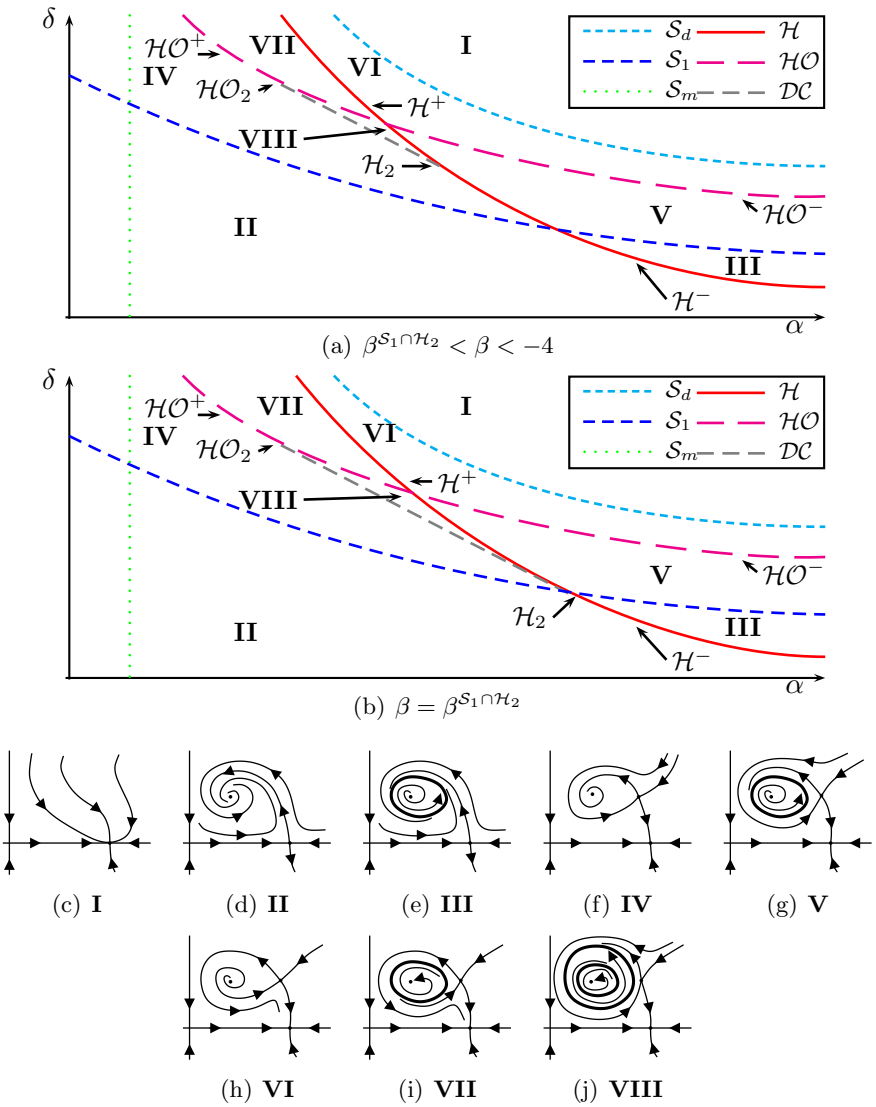

(a) $\beta^{\mathcal{S}_1 \cap \mathcal{H}_2} < \beta < -4$

(b) $\beta = \beta^{\mathcal{S}_1 \cap \mathcal{H}_2}$

(c) **I** (d) **II** (e) **III** (f) **IV** (g) **V**

(h) **VI** (i) **VII** (j) **VIII**

Figure 7.3: Bifurcation diagram and phase portraits for generic regions of parameters.

shape of the homoclinic bifurcation curve, $\mathcal{HO}$, is given by taking slices of Fig. 5.2 where μ_2 is constant. This yields the conjectured homoclinic bifurcation curve of Fig. 7.2, 7.3 and 7.4. We conjecture that the homoclinic bifurcation curve tends to infinity when $\beta \to -3$ (i.e. its left extremum point goes to infinity at $\beta = -3$). This comes from the fact that the region in which this curve may exist disappears (the region is created by the intersection of $\mathcal{H}$ and $\mathcal{S}_1$). This curve was confirmed numerically for $\beta = -3.5$ in section 8 (see Fig. 2(a)). The case $\beta = -4$ (see Fig. 2(b)) is partially obtained by taking the slice $\mu_2 = 0$ of the Fig. 5.2.

For the cases $\beta < -4$ the dynamics are much richer. In particular we conjecture the presence of a curve $\mathcal{DC}$ which represents the bifurcation of a double limit cycle.

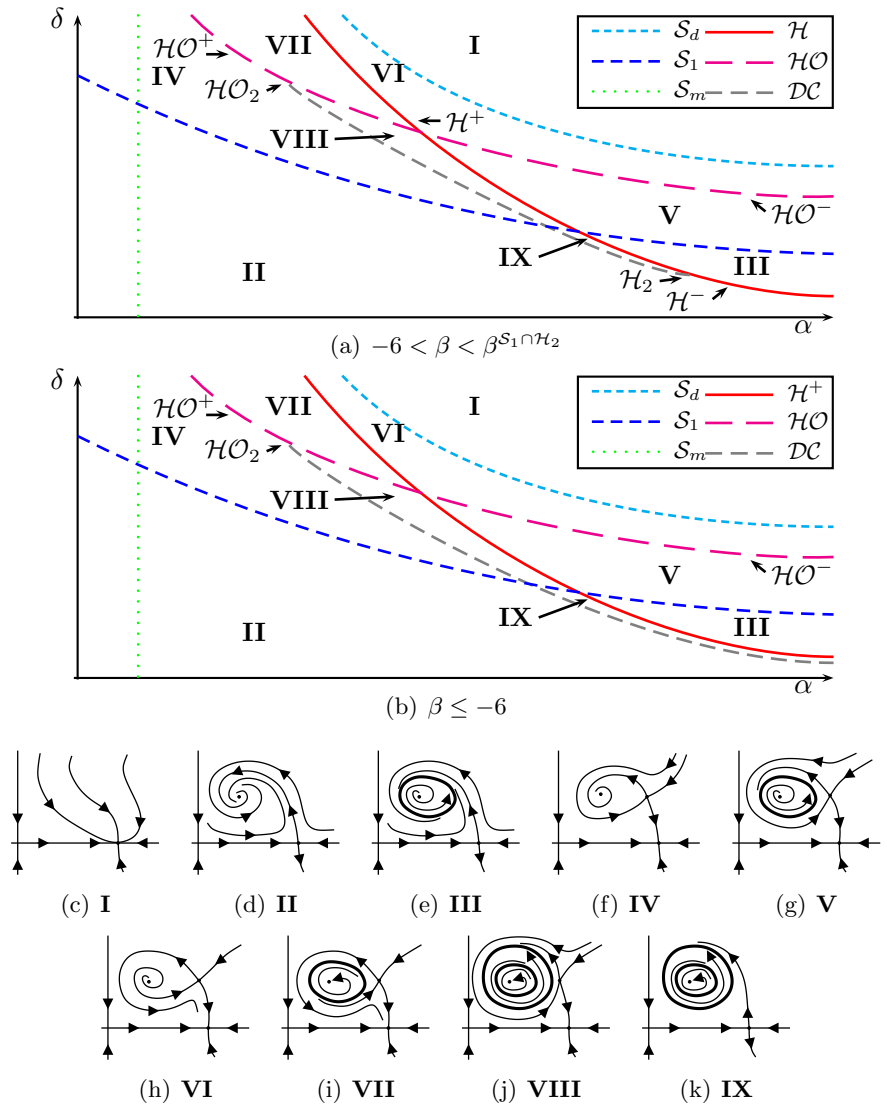

(a) $-6 < \beta < \beta^{\mathcal{S}_1 \cap \mathcal{H}_2}$

(b) $\beta \leq -6$

(c) **I** (d) **II** (e) **III** (f) **IV** (g) **V**

(h) **VI** (i) **VII** (j) **VIII** (k) **IX**

Figure 7.4: Bifurcation diagram and phase portraits for generic regions of parameters.

We have shown that it exists in a neighborhood of $\mathcal{H}_2$ and also in the unfolding of the Bogdanov-Takens bifurcation of codimension 3. The curve $\mathcal{DC}$ starts at $\mathcal{H}_2$ and ends at the homoclinic bifurcation of codimension 2, $\mathcal{HO}_2$. We conjecture that it is always the case. The $\mathcal{HO}$ exists in the neighborhood of the Bogdanov-Takens, near $\beta = -4$. Its extension is necessarily, negatively further from $\beta = -4$ to obtain a coherent bifurcation diagram. The main difference in the cases when $\beta < -4$ (see Fig. 6.3) is the position of $\mathcal{H}_2$ determined by $\alpha^{\mathcal{H}_2}(\beta) = \frac{\beta^2}{\beta+6}$ (see Proposition 6.8). The bifurcation point $\mathcal{H}_2$ will eventually cross $\mathcal{S}_1$ at $\beta = \beta^{\mathcal{H}_2 \cap \mathcal{S}_1} \approx -4.866$ and tend to infinity as $\beta \to -6$.

Remark 7.1 The bifurcation diagram presented here is the simplest which is compatible with all the constraints calculated so far. Since the bifurcation curves for the fixed points are exactly determined, the only conjectural curves are the curves $\mathcal{DC}$ and $\mathcal{HO}$. The existence and position of $\mathcal{DC}$ is guaranteed near $\mathcal{H}_2$ and $\mathcal{BT}_3$, while the existence and position of $\mathcal{HO}$ is known near $\mathcal{BT}$. The other bifurcation curves add additional constraints. For instance the curve $\mathcal{BH}$ can only occur when there are two singular points in the first quadrant. This shows that it always lie above $\mathcal{S}_1$. It also explains why it is expected to have disappeared for $\beta > -3$. Indeed for $\beta > -3$, the Hopf bifurcation only occurs when there is a unique singular point in the first quadrant.

8 Numerical Simulations and Homoclinic Bifurcation

For interesting fixed values of β, numerical bifurcation diagrams are given in the (α, δ) plane of the parameter space. When $\beta > 0$ we have taken the particular value $\beta = 6$ for which we have a generic numerical bifurcation diagram.

When $\beta < 0$ the values -3.5, -4, -5 of β are chosen to calculate the homoclinic orbit before, at the Bogdanov-Takens bifurcation of codimension 2 and 3 and after. Their choice allows to confirm numerically some of the conjectures of section 7. The Hopf bifurcation, $\mathcal{H}$, and the homoclinic bifurcation, $\mathcal{HO}$, are calculated using `XPPAUTO` in which some of the `AUTO` routines are integrated. The curve $\mathcal{HO}$ is calculated by taking a periodic solution of very large period and following it in the (α, δ) plane. This is one method to follow homoclinic bifurcation curves (see for instance [10]). The parameter ρ has an effect on the homoclinic bifurcation curve, $\mathcal{HO}$, but we conjecture that it has no effect on the topological bifurcation diagram. For ease of numerical computation we used $\rho = \frac{1}{100}$. This choice is based on the fact that, when ρ is larger, for many parameter values the vector field looks like a singular perturbation in at least one region of the first quadrant. The curves $\mathcal{S}_1, \mathcal{S}_d$ and $\mathcal{S}_m$ are directly computed with `MATLAB`.

The phase portraits were calculated with `ode45` of `MATLAB`. This is done by calculating the solutions forward and backward in time for intial values located on a equally spaced grid in the first quadrant. The grid size varies for best representation of the vector field. The hollow circles on the phase portrait represent the singular points.

8.1 A Typical Numerical Bifurcation Diagram for $\beta > 0$

The case $\beta = 6$ is a generic value and we obtain the numerical bifurcation diagram of Fig. 8.1. We also give the typical phase portraits at points a, b and c in Fig. 8.1. In Fig. 1(a) and Fig. 1(b), $(1, 0)$ is a saddle point and in Fig. 1(c), $(1, 0)$ is an attracting node. The phase portrait Fig. 1(a) (resp. Fig. 1(b)) has a singular point in the open first quadrant which is an attracting focus (resp. repelling focus), while Fig. 1(c) has no singular point in the open first quadrant. In addition, in Fig. 1(b) there is an attracting limit cycle around the singular point in the open

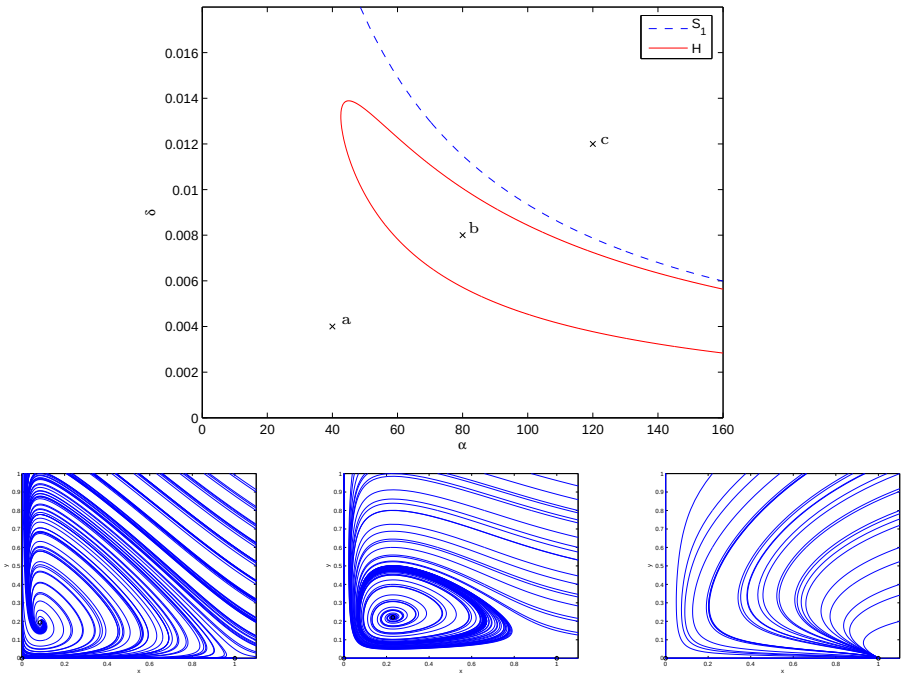

(a) no limit cycle (b) one limit cycle (c) no limit cycle

Figure 8.1: Numerical bifurcation diagram and phase portraits ($\beta = 6$).

first quadrant. We notice that the numerical bifurcation diagram and numerical phase portraits confirm the results established by the theory.

8.2 Numerical Simulations of the Homoclinic Orbit Bifurcation

The case $\beta = -3.5$ is a generic value and we obtain the numerical bifurcation diagram of Fig. 8.2. This diagram confirms the 'c' shape of $\mathcal{HO}$, conjectured in Fig. 2(a), with the help of Fig. 5.2. Therefore, numerically, it is observed that $\mathcal{HO}$ extends at least to $\beta = -3.5$. We conjectured that the curve will disappear towards the right (the left extremal point tends to infinity) as β tends to -3. We give a representation of different phase portraits in Fig. 8.3 for values a, b, c and d appearing in Fig. 2(b). In all the examples of phase portraits the singular point $(1, 0)$ is an attracting node and the left singular point (resp. right singular point) is a repelling focus (resp. saddle point). The examples show the change in the gobal behavior of the system from: attracting limit cycle to homoclinic orbit, to no limit cycle, and back to a limit cycle. We also notice that some of the phase portraits are similar to those observed in singular perturbations: we explore this phenomenon in section 8.3. We discuss the biological interpretation in section 9.

The case $\beta = -4$ is where we find the Bogdanov-Takens bifurcation of codimension 3: indeed it is observed numerically that $\mathcal{HO}$ and $\mathcal{H}$ meet at $(\alpha, \delta) = (8, \frac{1}{4})$. This confirms the behavior of Fig. 2(b) predicted by Fig. 5.2 when $\mu_2 = 0$. We

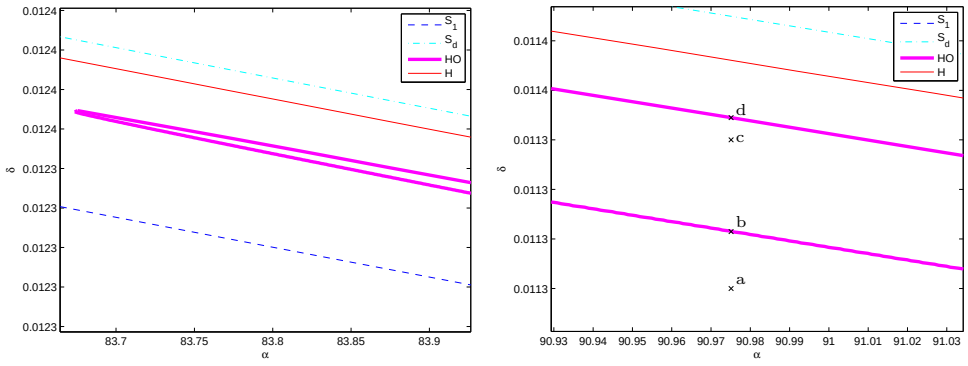

(a) 'c' shape of $\mathcal{HO}$ (b) zoom of the diagram

Figure 8.2: Numerical bifurcation diagram ($\beta = -3.5$).

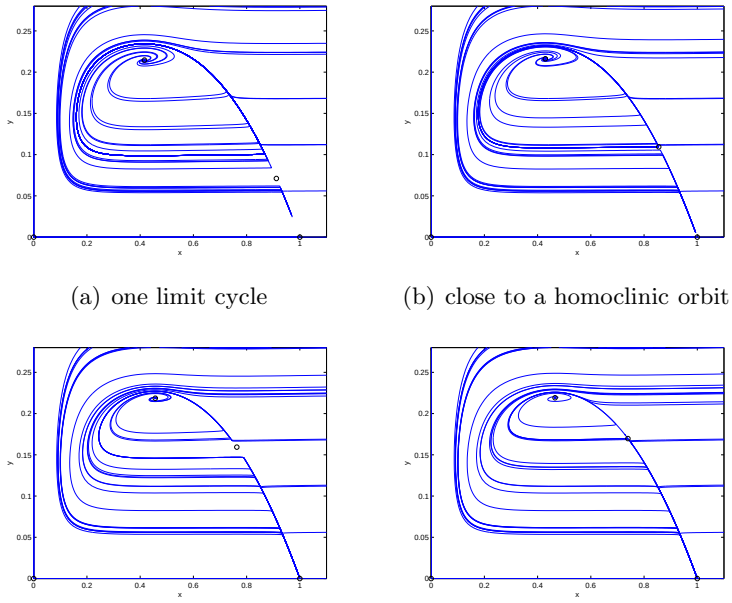

(a) one limit cycle (b) close to a homoclinic orbit

(c) no limit cycle (d) close to a homoclinic orbit

Figure 8.3: Phase portraits ($\beta = -3.5$).

give a representation of some phase portraits in Fig. 8.4. The singular point $(1, 0)$ in Fig. 4(c) is a saddle point and for all other cases it is an attracting node. In Fig. 4(a) and 4(c) the left singular point is an attracting focus, while in the remaining cases the left singular point is a repelling focus when it exists. In all cases the right singular point is a saddle point when it exists.

The case $\beta = -5$ is more complex since there is a Hopf bifurcation of codimen-

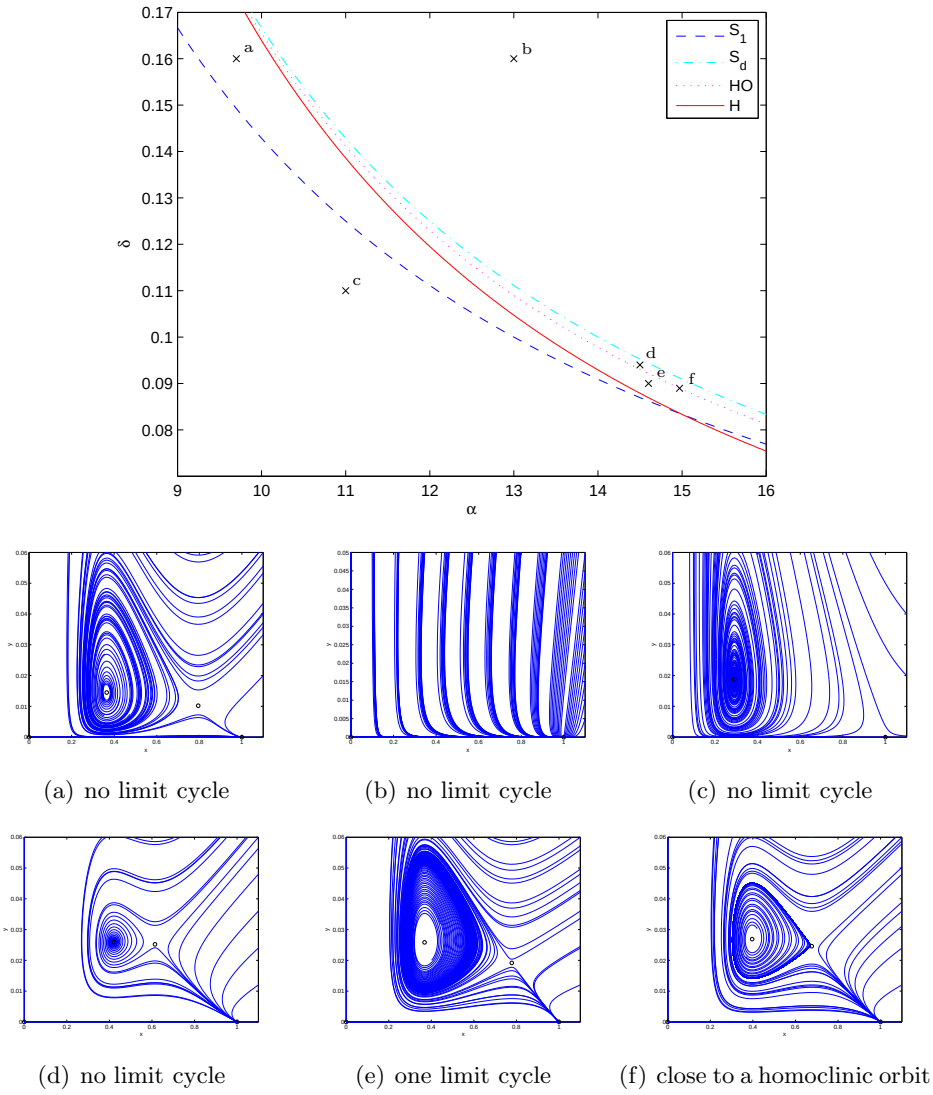

(a) no limit cycle (b) no limit cycle (c) no limit cycle

(d) no limit cycle (e) one limit cycle (f) close to a homoclinic orbit

Figure 8.4: Zoom of the numerical bifurcation diagramme and phase portraits ($\beta = -4$).

sion 2, $\mathcal{H}_2$, as predicted by the theory. While we could not numerically compute $\mathcal{DC}$ which represents a double limit cycle, we give evidence that it exists locally in a neighborhood of $\mathcal{H}_2$. Indeed we are able to find parameter values for which there are two limit cycles around the singular point which undergoes the Hopf bifurcation. The external limit cycle is attracting and the internal limit cycle is repelling, as predicted by the theory. See Fig. 5(c). We had conjectured that $\mathcal{DC}$ begins at $\mathcal{H}_2$ and ends at the homoclinic bifurcation of codimension 2, $\mathcal{HO}_2$. The existence of $\mathcal{HO}_2$ is confirmed by the numerical existence of both a repelling homoclinic orbit and an attracting homoclinic orbit. In section 8.4 we compute

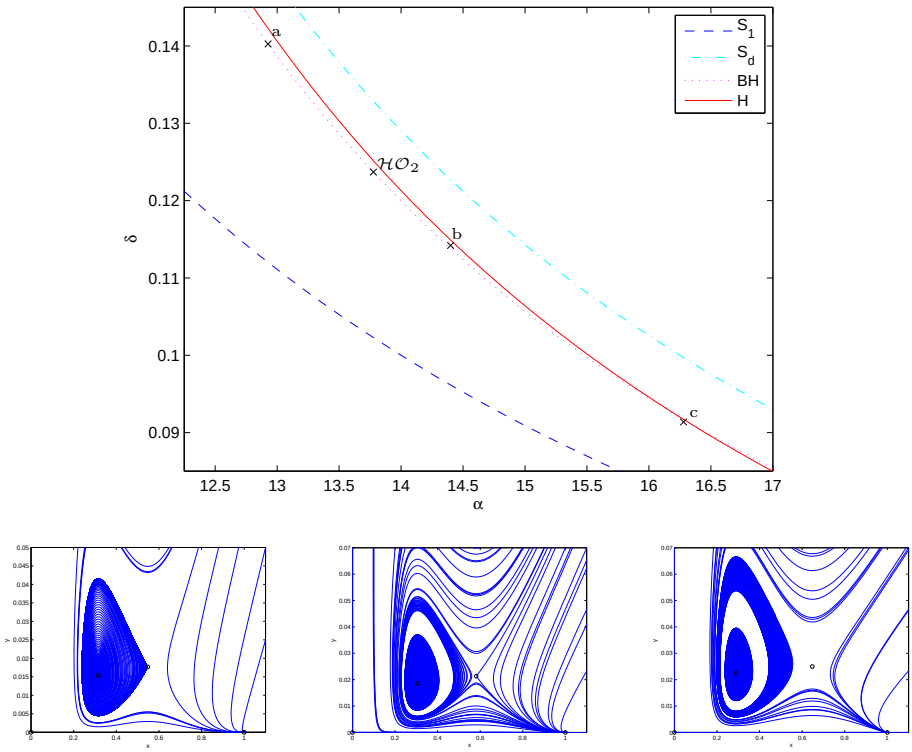

(a) close to a homoclinic orbit (b) a limit cycle (c) two limit cycles

Figure 8.5: Zoom of the numerical bifurcation diagram and phase portraits ($\beta = -5$).

the location of $\mathcal{HO}_2$, in particular when $\beta = -5$, its location is given in Fig. 8.5. See Fig. 5(a), where the phase portrait shows a repelling homoclinic. In all three phase portraits of Fig. 8.5 the singular points have the same type: $(1, 0)$ is an attracting node, the left singular point is an attracting focus, and the right singular point is a saddle.

8.3 Condition of Existence of an Homoclinic Orbit in the Limit Case of a Singular Perturbation

The system is a singular perturbation if the family of vector fields has the following form

$$\begin{aligned} \dot{x} &= \rho x(1-x) - \frac{yx^2}{\alpha x^2 + \beta x + 1} \\ \dot{y} &= \epsilon(x, \alpha, \beta, \delta) y \end{aligned} \tag{8.1}$$

where $\epsilon(x, \alpha, \beta, \delta)$ is very small for $x \in (a - \gamma_1, b + \gamma_2)$, with $\gamma_1 \in (0, a)$ and γ_2 is sufficiently large, where a and b are defined in Fig. 6(a). This implies that the

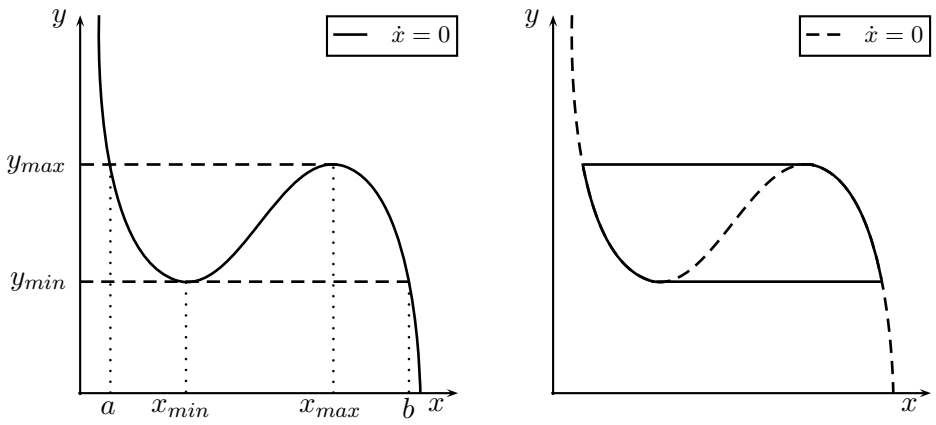

(a) Nullcline of $\dot{x}$ (b) Limit cycle

Figure 8.6: Vector field in the limit case of a singular perturbation.

vector field is nearly horizontal far from the nullcline of $\dot{x}$. If the system (8.1) has a limit cycle, it will have the appearance of the limit cycle shown in Fig. 6(b). If the vector field is of the form (8.1) then there exists a homoclinic orbit at the limit case (i.e. $\epsilon(x, \alpha, \beta, \delta)$ vanishing) when the singular point of saddle type is approximately located at (b, y_{min}).

It is possible to compute in the parameter space, the surface which represents the homoclinic orbit in the limit case of a singular perturbation.

Theorem 8.1 *If a family of vector fields of the form* (8.1) *has a homoclinic orbit, then at the limit (when* $\epsilon(x, \alpha, \beta, \delta) \to 0$*) the parameters satisfy* $H(\alpha, \beta, \delta) = 0$ *where*

$$\begin{aligned} H(\alpha,\beta,\delta) = {} & (\alpha^6 + 2\alpha^5 b + 2\alpha^5 + 2\alpha^4 b + \alpha^4 + \alpha^4\beta^2)\delta^3 \\ & + (2\alpha^2\beta^3 - 2\alpha^5 - 18\alpha^4 - 2\alpha^4\beta - 16\alpha^3\beta + 2\beta^2\alpha^3 - 2\beta^2\alpha^2)\delta^2 \\ & + (\alpha^4 + 32\alpha^3 + 16\alpha^2\beta - 2\beta^2\alpha^2 + \beta^4)\delta - 16\alpha^2. \end{aligned} \tag{8.2}$$

Proof. Let $y(x)$ be the nullcline of $\dot{x}$ then x_{min} is a solution of $y'(x) = 0$. We look for the condition for which a local minimum (x_{min}, y_{min}) of the nullcline $\dot{x}$ has the same y coordinate as the saddle (x_0, y_0), that is $d(x_{min}, x_0) = y(x_{min}) - y(x_0) = 0$. We want to obtain a condition in the parameter space, therefore we take the resultant R of the numerator of $d(x_{min}, x_0)$ and $f(x_0)$ (where f is given in (3.3)) with respect to x_0. We proceed to take the resultant of R and the numerator of $y'(x_{min})$ with respect to x_{min}. We obtain $\alpha^2\rho^{12}P(\alpha, \beta, \delta)^2 H(\alpha, \beta, \delta)$ where $P(\alpha, \beta, \delta)$ is given in (6.2) and $H(\alpha, \beta, \delta)$ given in (8.2). The factor $P(\alpha, \beta, \delta)^2$ has already been studied and its solution branch does not represent a homoclinic orbit: it corresponds to the case $x_{min} = x_0$. □

Fig. 8.7 gives two examples with the nullcline of $\dot{x}$ superposed with solution(s). Fig. 7(a) gives a phase portrait which is not singular, while Fig. 7(b) is the phase

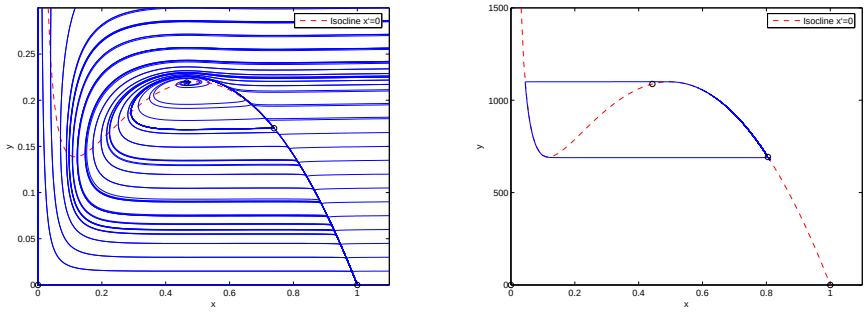

(a) Not a singular perturbation vector field (b) Singular perturbation vector field

Figure 8.7: Examples of vector fields with a homoclinic orbit.

β	α	δ	ρ	Fig.
-3.5	90.9751	0.0113545	$\frac{1}{100}$	7(a)
-3.5	90.9751	0.01134173	50	7(b)

Table 2: Parameter values for the examples of Fig. 8.7.

portrait of a singular perturbation vector field whose parameters satisfy the function $H(\alpha, \beta, \delta) = 0$. The parameters of both examples are given in Tab. 2.

8.4 Homoclinic Orbit of Codimension 2

The existence of a Bogdanov-Takens bifurcation of codimension 3 implies that there exists, in a neighborhood of that bifurcation, a curve in the parameter space for which there is a homoclinic bifurcation of codimension 2, $\mathcal{HO}_2$. It is difficult to find the location of $\mathcal{HO}_2$ in the parameter space but, if $\mathcal{HO}$ were known, then only a local additional condition is necessary to find $\mathcal{HO}_2$, namely the trace of the Jacobian at the saddle vanishes. We have seen in section 6 that the trace of the Jacobian vanishes at a singular point (x_0, y_0) precisely when $P(\alpha, \beta, \delta) = 0$ where P is given in (6.2). Let $(\alpha^{\mathcal{HO}_2}(\beta, \rho), \delta^{\mathcal{HO}_2}(\beta, \rho))$ be the coordinate of $\mathcal{HO}_2$ in the parameter space which satisfies $P(\alpha^{\mathcal{HO}_2}(\beta, \rho), \beta, \delta^{\mathcal{HO}_2}(\beta, \rho)) = 0$.

Proposition 8.2 *If $\beta < -4$ and ρ are fixed then the point $\mathcal{HO}_2$ in the parameter space is such that $\alpha^\infty = 1 - \beta < \alpha^{\mathcal{HO}_2}(\beta, \rho)$.*

Proof. This follows directly from the fact that the solution branch of $P(\alpha, \beta, \delta) = 0$ (see (6.2)) which represents the zero trace saddle tends to infinity with respect to δ as α tends to $\alpha^\infty = 1 - \beta$. In Fig. 8.8 we have added to the bifurcation diagram a curve $\mathcal{SP}$ which represents the solution branch of $P(\alpha, \beta, \delta) = 0$ attached to the zero trace saddle. □

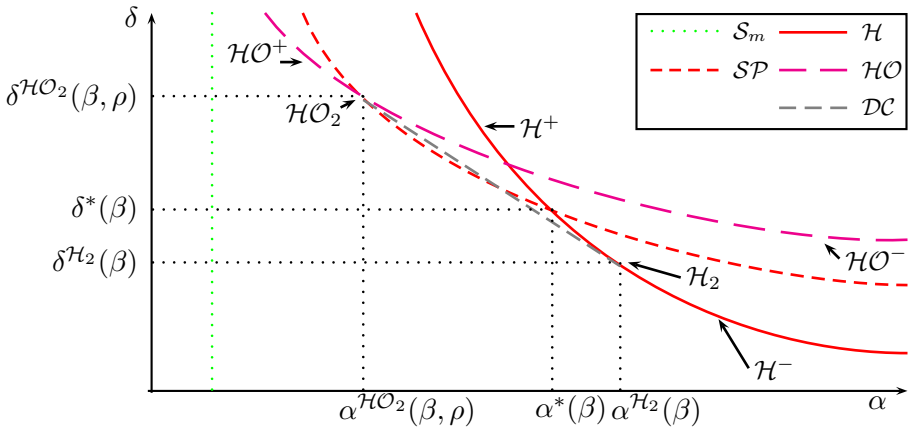

Figure 8.8: Diagram of the curves $\mathcal{SP}$, $\mathcal{H}$ and $\mathcal{HO}$ for $-6 < \beta < -4$.

β	$\frac{\beta^2}{4}$	$\alpha^{\mathcal{HO}_2}(\beta,\rho)$	$\alpha^*(\beta)$	$\alpha^{\mathcal{H}_2}(\beta)$
-4.1	$\frac{1681}{400} = 4.2025$	8.5055	$\frac{52111}{6100} \approx 8.5428$	$\frac{1681}{190} \approx 8.8474$
-5	$\frac{25}{4} = 6.25$	13.7771	$\frac{100}{7} \approx 14.2857$	25
-6	9	20.8609	$\frac{45}{2} \approx 22.5$	does not exist
-10	25	62.6862	75	does not exist

Table 3: Numerical simulation of the α-coordinate of $\mathcal{HO}_2$ where $\rho = \frac{1}{100}$.

We conjecture a better lower bound $\frac{\beta^2}{4} < \alpha^{\mathcal{HO}_2}(\beta,\rho)$ and also that $\alpha^{\mathcal{HO}_2}(\beta,\rho) \to \infty$ as $\beta \to -\infty$. This is based on numerical simulations given in Tab. 3.

9 A Biological Interpretation

The biological interpretation that can be directly observed from the conjectured bifurcation diagram is for a family of systems such that k, c and m are constant. That is we suppose that the carrying capacity of the prey, k, is constant, the efficiency of the predator to convert prey into predator, c, is constant and that the fitting parameter $m = \frac{p''(0)}{2}$ which partially controls the limit of the response function when it tends to infinity is constant.

Hence, if the parameter δ changes, this implies that the death rate d changes linearly since $\delta = \frac{d}{cmk^2}$. Similarly, if α changes it implies that a changes linearly since $\alpha = ak^2$. The parameter a partially controls the limit, L, and the 'hump', M, of the response function when b is negative (i.e. as a increases the limit, L, decreases and the 'hump', M, will also decrease). This can be interpreted as the predator being less effective against the prey.

Under the above assumptions we discuss a few dynamics of the populations under different values of parameters. For all fixed β, we can assert the following

two observations. We notice that if the death rate, δ, of the predator increases, this will eventually result in the extinction of the predator. Similarly, if α increases, then the predator will become extinct. Both of these statements are intuitively sound.

In the case $\beta \geq -2$, there are three possibilities of stable regimes for the populations in the long term: extinction of the predator (no singular point in the open first quadrant, see **I**), oscillating populations of predator and prey (stable periodic solution, see **III**), or constant populations (attracting singular point in the open first quadrant, see **II**). The effect of the group defence on the phase portraits and on the bifurcation diagrams for fixed β can only be seen for β sufficiently negative.

The case $\beta < -2$ has much richer dynamics partially caused by the possibility of a second equilibrium in the open first quadrant. Indeed for fixed values of the parameters different stable regimes are possible depending on the initial conditions. For instance, if $\beta \in [-3, -2)$ (see Fig. 1(d)) in region **IV**, the system will have the possibility of two stable regimes depending on the initial condition, one with the predators extinct and one with co-existing populations.

A more special case is for $\beta \in (-4, -3)$ (see Fig. 2(a)): if α is fixed at a sufficiently large value, starting with δ sufficiently small and increasing δ, the stable regime of the system will change in the following manner:

- stable equilibrium of co-existing populations (attracting singular point, see **II**),
- stable oscillation of the populations (stable limit cycle, see **III**),
- two stable regimes: a stable oscillation of the populations (stable limit cycle) and one with extinction of the predator, depending on the initial condition (see **V**),
- extinction of the predator (following the annihilation of the limit cycle through the homoclinic orbit, passage from **V** to **VI**).

At this point a peculiar phenomenon occurs, if δ (death rate of the predator) increases the predator has the possibility of not becoming extinct for good initial conditions. This is caused by the global behavior of the system: the homoclinic orbit, creates a limit cycle: for initial conditions inside that limit cycle the stable regime is the stable oscillation of populations. The same suprising results has been observed in the study of the Holling generalised function of type IV [24]. This global phenomenon can only happen with a response function which is non-monotone. We conclude in asking if there is a biological interpretation for such a phenomenon which seems counter-intuitive.

Acknowledgments

We are very grateful to Huaiping Zhu for suggesting the topic and for several helpful discussions, in particular considering the Hopf bifurcation of codimension

2.

References

[1] J. F. Andrews, *A mathematical model for the continuous culture of microorganisms utilizing inhibitory substrates*, Biotechnology and Bioengineering, Vol. 10, 707–723, 1968.

[2] R. I. Bogdanov, *Versal Deformation of Singularity of a Vector Field on the Plane in the Case of Zero Eigenvalues*, Selecta Mathematica Sovietica, Vol. 1, 4 (1981), 389–421.

[3] G. Bonin & J. Legault, *Comparaison de la méthode des constantes de Lyapunov et de la bifurcation de Hopf*, Canad. Math. Bull., Vol. 31 (2), (1988), 200–209.

[4] H. W. Broer, V. Naudot, R. Roussarie, K. Saleh, *A predator-prey model with non-monotonic response function*, Regul. Chaotic Dyn., Vol. 11 (2006), 155-165.

[5] H. W. Broer, V. Naudot, R. Roussarie, K. Saleh, *Dynamics of a predator-prey model with non-monotonic response function*, Disc. Cont. Dyn. Sys., Vol. 18 (2007), 221-251.

[6] M. Caubergh & F. Dumortier, *Hopf-Takens bifurcations and centres*, Journal of Differential Equations, Vol. 202 (2004), 1–31.

[7] C. Chicone, *Ordinary Differential Equations with Applications*, Springer-Verlag, New York, 1999.

[8] C. Coutu, *Étude du diagramme de bifurcation d'un système prédateur-proie*, Mémoire de maîtrise, Université de Montréal, 2003.

[9] S.-N. Chow, C. Li & D. Wang, *Normal Forms and Bifurcation of Planar Vector Fields*, Cambridge University Press, New York, 1994.

[10] E. J. Doedel, H. B. Keller and J.-P. Kernevez, *Numerical analysis and control of bifurcation problems (II): bifurcation in infinite dimensions*, International Journal of Bifurcations and Chaos, Vol. 1 (1991), 745–772.

[11] F. Dumortier, R. Roussarie & J. Sotomayor, *Generic 3-parameter families of vector fields on the plane, unfolding a singularity with nilpotent linear part. The cusp case of codimention 3*, Ergodic Theory Dynamical Systems, Vol. 7 (1987), no 3, -375–413.

[12] H. I. Freedman, *Stability Analysis of a Predator-Prey System with Mutual Interference and Density-Dependent Death Rates*, Bulletin of Mathematical Biology, Vol. 41, 67–78, 1979.

[13] H. I. Freedman, *Deterministic Mathematical Models in Population Ecology*, Marcel Dekker, Inc, New York, 1980.

[14] H. I. Freedman & G. S. K. Wolkowicz, *Predator-prey Systems with Group Defence: the Paradox of Enrichment Revisited*, Bulletin of Mathematical Biology, Vol. 48, No 5/6, 493–508, 1986.

[15] G. F. Gause, *The Struggle for Existence*, Hafner Publishing Company, New York, 1969.

[16] F. Göbber & K.-D. Willamowski, *Ljapunov Approach of Multiple Hopf Bifurcation*, Journal of Mathematical Analysis and Applications, Vol. 71, 333–350, 1979.

[17] J. Guckenheimer & P. Holmes, *Nonlinear Oscillations, Dynamical Systems, and Bifurcations of Vector Fields*, Springer-Verlag, New York, 1983.

[18] C. S. Holling, *The Functional Response of Predators to Prey Density and its Role in Mimicry and Population Regulation*, Memoirs of the Entomological Society of Canada, Vol. 45, 3–60, 1965.

[19] J. L. Jost, J. F. Drake, A. G. Fredrickson & H. M. Tsuchiya, *Interactions of Tetrahymena pyrisformis, Escherichia cole, Azotobacter vinelandii, and Glucose in a Minimal Medium*, Journal of Bacteriology, Vol. 113, 834–840, 1973.

[20] J. L. Jost, J. F. Drake, H. M. Tsuchiya & A. G. Fredrickson, *Microbial Food Chains and Food Webs*, Journal of Theoretical Biology, Vol. 41, 461–484, 1973.

[21] Y. Lamontagne, *Étude d'un système prédateur-proie avec fonction de réponse Holling de type III généralisée*, Mémoire de maîtrise, Université de Montréal, 2006.

[22] S. Ruan & D. Xiao, *Global Analysis in a Predator-Prey System with Nonmonotonic Functional Response*, SIAM Journal of Applied Mathematics, Vol. 61, No 4, 1445–1472, 2001.

[23] G. S. K. Wolkowicz, *Bifurcation Analysis of a Predator-Prey System Involving Group Defence*, SIAM Journal of Applied Mathematics, Vol. 48, No 3, 592–606, 1988.

[24] H. Zhu, S. A. Campbell & G. S. K. Wolkowicz, *Bifurcation Analysis of a Predator-Prey System with Nonmonotonic Functional Response*, SIAM Journal of Applied Mathematics, Vol. 63, No 2, 636–682, 2002.